FLOW SIMULATION IN SHALE GAS RESERVOIRS

Submitted by

Mahmoud Younes

Department of Environment, Land and Infrastructure Engineering

In partial fulfillment of the requirements

For the Degree of Master of Science in Petroleum Engineering

Politecnico Di Torino

Turin, Italy

December 2018

Advisor: Vera Rocca

Acknowledgements

I am very thankful to my supervisor, professor Vera Rocca, whose expertise, understanding, generous guidance and support made it possible for me to work on a topic that was of great interest to me. It was good working with her.

I would also like to thank Kappa Engineering for the huge amount of support provided throughout the work on the simulations part of my thesis, from the fast responses to my support requests, tutorials made available online and the evaluation license provided to be able to use the Kappa Workstation simulator on my own personal PC.

I gratefully acknowledge the support provided by professor Kamy Sepehrnoori from the University of Texas at Austin regarding some aspects of the simulations and supplying related research work from one of his students.

I would like to express my sincerest love and gratitude to my family back home, my parents Hassan and Rania and my sisters Sali and Jessy for their unflagging support, encouragement and endless love, throughout my studies. To my uncle, Ali Madi, whose unconditional love and support was one of the reasons I got this far. To the souls of my grandmother Hadiyah and grandfather Mustafa, I dedicate this work.

Finally, I would like to thank all those who helped and inspired me throughout my studies and research.

Abstract

A higher energy demand in the last decades has played a substantial role in the insistent investigation and exploration of unconventional oil and gas resources. Shale gas reservoirs are amongst the major unconventional resources. These resources defer from conventional ones in such a way that they cannot be produced and developed by conventional techniques relying only on the pressure difference and other normal operations like pumping or compression. Technological advancement in both horizontal drilling and hydraulic fracturing methods have been the key to attain economical production rates and recovery factor from shale gas reservoirs. Shale gas reservoirs have a relatively small permeability , in the range of 10^-4 mD, and are known for their complex gas transport mechanisms as well as the complex natural and induced hydraulic fracture geometries and network. Typical shale gas production is composed mostly of two-phase flow of gas and water. However, suitable modeling of the two-phase behavior while also incorporating the much more complex fracture geometries and properties have been a challenge within the industry.

In this research, a 3D synthetic reservoir model is constructed using the commercial simulator Rubis by Kappa Engineering. Via the fluid flow numerical simulation approach, the effects of different levels of hydraulic as well as natural fracture complexities(considering geometry, network and petrophysical characteristics, both single and two-phase flow) were investigated in terms of the overall well performance and production, and, consequently, system recovery factor.

On one hand, it was shown how both induced hydraulic and natural fracture geometries and distribution resulted in a different stimulated reservoir volume and thus affecting the final recovery mostly due to extent of interference between individual fractures. On the other hand, how much water injected before production, which was expressed in the relative permeability curves (Water Saturation) inside the fractures, reached a point where no further increase in recovery can be achieved. Furthermore, the fractures' conductivity affected production only after falling below 1 mD.ft.

The research results confirm the key role played by a proper modeling of the fracture network, and how much it can interfere with the results of gas and water production.

Moreover, it displays a better understanding of the ideal water injection during the beginning of production to optimize the final recovery and avoid a high water flow-back. In addition to explaining at what values the fracture conductivities and angles cause the highest disruption in production.

Table of Contents

List of Figures

List of Tables

Chapter 1: Introduction

1.1 Background

According to an initial assessment made by the Energy Information Administration (EIA) in 2013, there is an estimated 7,576 trillion cubic feet of technically recoverable wet shale gas in the world (1). This compared to about 6,650 tcf of proven gas reserves (2) , shows that shale gas is likely to become a noteworthy source of natural gas and subsequently increase the overall natural gas production around the world. Figure 1 shows the assessed worldwide shale basins based on some criterion and following a methodology set by the EIA.

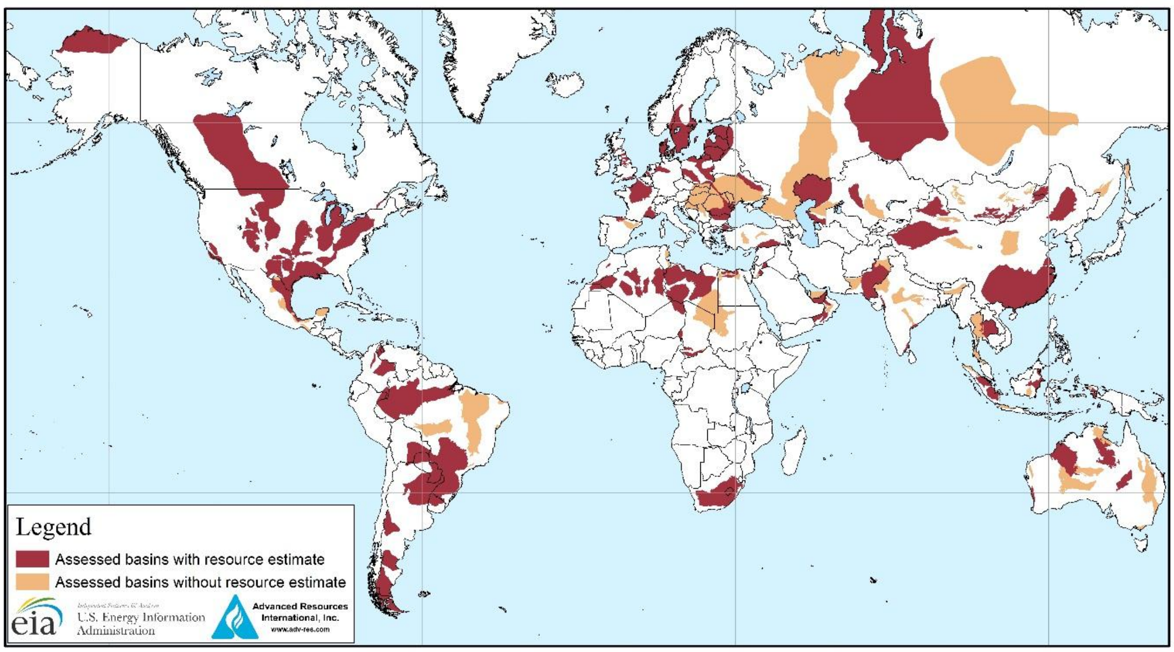

Figure 1: Map of assessed shale basins (EIA,2014)

In the International Energy Outlook (IEO, 2016) and the Annual Energy Outlook (AEO, 2016), natural gas production worldwide is projected to increase from 342 billion cubic feet per day (Bcf/d) in 2015 to 554 Bcf/d in 2040 with shale gas increasing from 42 Bcf/d in 2015 to 186 Bcf/d in 2040. Shale gas, having increased in more than 340%, will account of up to 30% of the total natural gas produced by 2040 as shown in figure 2 (3).

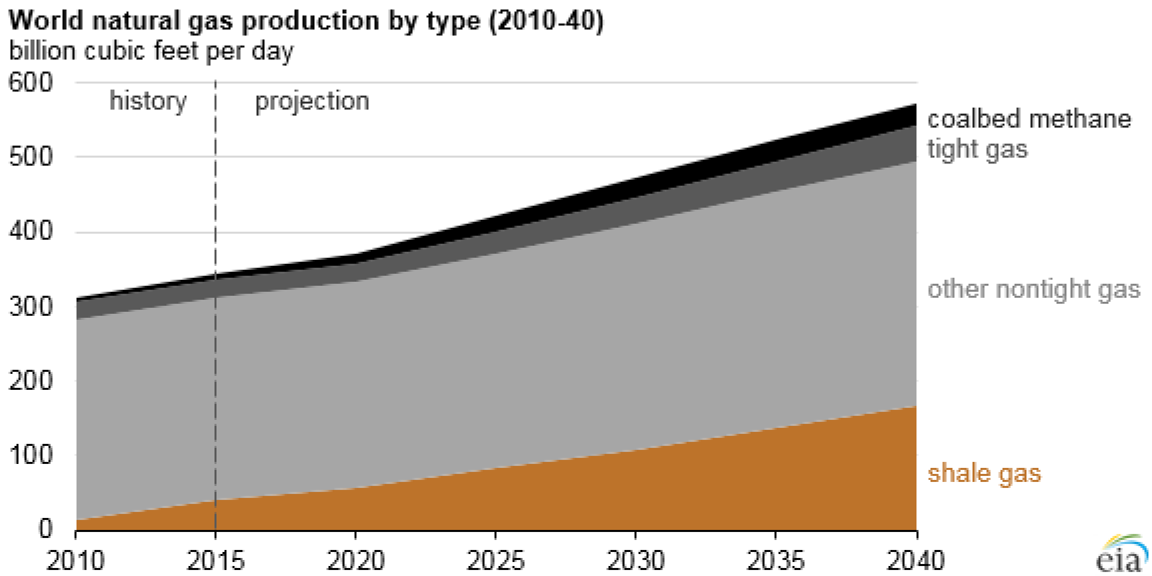

Figure 2: World Natural Gas Production by Type (2010-2040)

As compared to conventional resources, shale requires a more challenging development. For instance, a recovery factor between 20-40% for Marcellus shale in the US has been observed. However, this can be enhanced by further stimulation and varies depending on the reservoir's geology, current market prices and how accessible the reservoir is. On the other hand, conventional resources can have similar recovery factors and, in some cases, even more but with way lower development and production costs which makes it more favourable. (4)

Currently, only 4 countries produce shale gas. In addition to the United States, Canada, China and Argentina, also Algeria and Mexico are expected to join as the largest commercial shale gas producers in the near future. The 6 countries together will account for 70% of the worldwide shale production by 2040. As we can notice in the figure 3, shale gas dominates as the main source of natural gas in some of the mentioned countries due to the forecasted reduced costs of development and production and technological improvements, with Mexico and Argentina reaching 75% in shares (3). China is also expected to have a substantial increase in the percentage of its gas coming from shale sources. With the US continuing its current trends, it is also expected to bypass 60% in shale gas production by 2040.

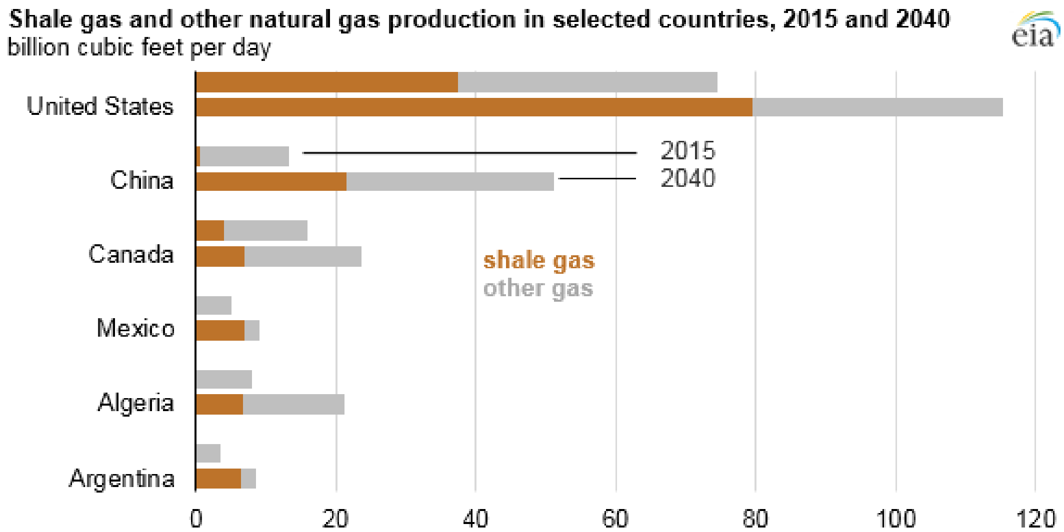

Figure 3: Shale gas and other natural gas production in selected countries (2015/2040)

Natural gas is one of the major energy sources used globally. The demand of energy from this source is increasing because it is seen as more environmentally friendly than oil. Recent innovative technologies have allowed for more natural gas development from unconventional resources like tight gas and oil, coalbed methane and shale gas.

When considering conventional resources only, about 61% of natural gas reserves are found in the middle east and Eurasia opposed by only 4% (283Tcf) in the United States. When unconventional resources are added, the recoverable gas in the united states increase to almost 2074Tcf with shale gas accounting to about 36% of those reserves.

As the technology required to develop these unconventional resources has advanced, the amount of recoverable reserves have improved. However, we still don't quite understand these low-permeability formations. More knowledge in this area is needed which would lead to a more cost-efficient development worldwide. The next chapter will discuss more about how these formations are developed, produced and how gas transport mechanics work.

1.2 Research objective

The objective of this research is to properly compare and provide an understanding of the effect of fracture geometries on the well performance and Recovery Factor. A simple shale gas reservoir is modelled, and then multiple cases of hydraulic fractures are added to wells. These cases can range from simple planar fractures to a more complex fracture distribution. This will help us better understand the behaviour of shale gas reservoirs and consequently optimise production strategies. The main points addressed in this thesis can be summarised as follows:

- Develop a numerical model of a shale gas reservoir considering one single well and multiple induced hydraulic fractures, based on typical fluid and reservoir properties of shale gas reservoirs from technical literature, while incorporating complex aspects of shale gas transport mechanisms like gas adsorption and slippage.
- Simulate different cases of induced hydraulic fracture geometries in a 3D model to better understand their effects on both single phase (Gas) and 2-Phase (Gas and Water) flow performance of the well.
- Simulate some cases of natural fractures which differs in terms of fracture number and orientation in the reservoir model and study the flow performance as well.
- Examine how the reservoir and fracture properties (Swi and K) can affect the 2-Phase performance of the well by conducting a sensitivity analysis.

1.3 Thesis Outline

The thesis contains 5 chapters which thoroughly explain the topic.

Chapter 1 begins with a background on global shale gas production and comparing it with conventional gas reserves while also providing a forecast of estimated shale gas production in the forthcoming years. It finally shows the main objectives of this research.

The second chapter briefly clarifies the difference between the 2 types of shale focusing mainly on shale gas. It later explains hydraulic fracturing, which is the main method used for production in shale gas and it summarises typical recovery and production data. Finally, it presents the current approaches used in the industry to simulate shale gas reservoirs and fracturing using commercial simulators.

Chapter 3 discusses the commercial simulator used to run the simulations and states some equations considered to govern for typical gas behaviour. Moreover, the shale gas reservoir model used in the simulations will be introduced alongside a thorough presentation of the reservoir parameters and the considered fracture scenarios.

The fourth chapter displays all the results of the simulations in graphs, tables and also 3D maps of the reservoir. It compares the cases simulated and further on analyzes the results to show the effect of the fracture geometries on the flow and production. A forecast also shows the reservoir performance over the next few years. In the end Swi and the fracture's conductivity is changed to present a sensitivity analysis.

To end, chapter 5 recaps all the results and presents a conclusion of the findings.

Chapter2: Literature Review

2.1 Unconventional Resources

Oil and Natural gas resources that generally require more complicated and specialized production and extraction techniques are called unconventional resources. These resources are positioned in a geological way where normal extraction is not possible. Generally speaking, the structure and fluid properties does not allow for conventional extracting and production methods and thus requires more costly methods and technological advancements (5).

At present, porosity, fluid trapping mechanisms, permeability and other characteristics that differ from sandstone and carbonate are used to classify resources as conventional or not. (6)

Typical unconventional resources include, among others, gas hydrates, heavy oil reservoirs, coalbed methane and tight gas sands, gas and oil shale reservoirs.

In particular, gas and oil shale resources defer from conventional ones in such a way that they cannot be produced and developed by conventional techniques relying only on the pressure of the well and other normal operations like pumping or compression. These resources are trapped in sediments of rock called shale. Shale is a type of sediment characterized by very low values of permeability (typically in ranges below 0.0001 mD) and porosities below 6% which makes it difficult to liberate the tiny particles of hydrocarbons without proper stimulation.

Before the 2000, oil and gas prices were at somehow low levels to allow for the research and development of unconventional resources. However, as hydrocarbon prices increased after 2000 and the realization by major oil and gas producers by the abundant shale availability and prospect in their countries, more research was made for the development of these fields. This has allowed to explore and produce some of the largest natural gas deposits in the world.

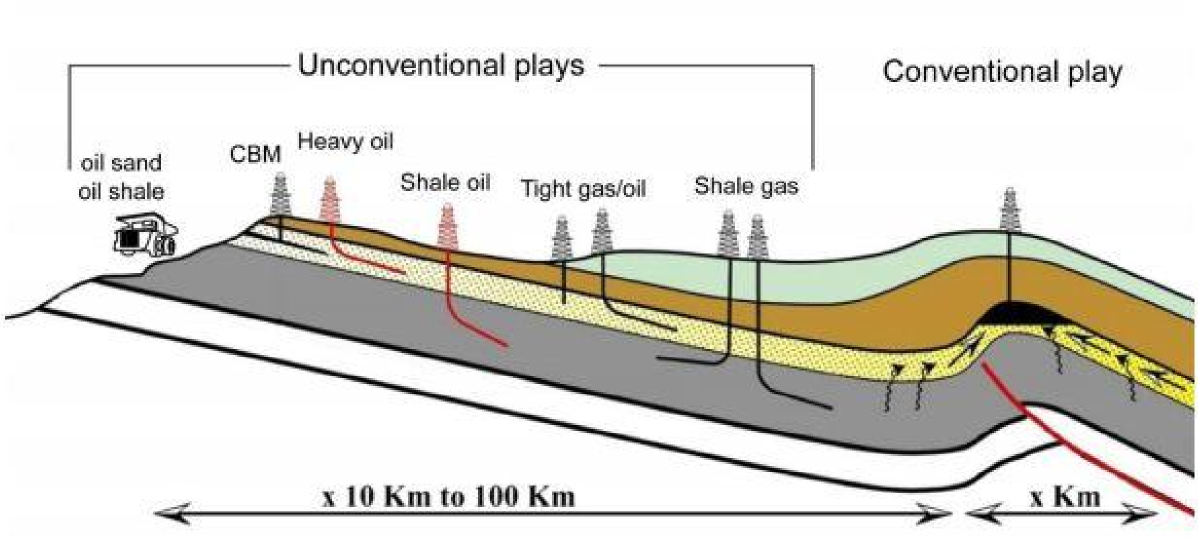

Figure 4: Different Types of Unconventional Plays (modified after IFPEN 2010)

The most accurate definition which takes into account both reservoir and fluid properties are shown in the figures below.

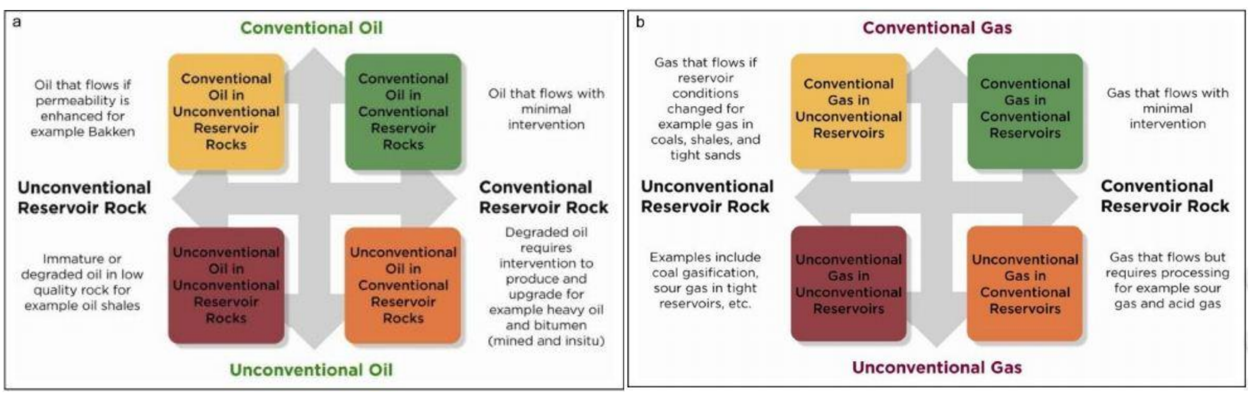

Figure 5: Classification of (a) Oil and (b)Gas resources based on Reservoir and Fluid Properties

2.1.1 Shale Gas

In conventional hydrocarbon resources, a source rock, a reservoir and a trap as three separate components should be present within a specific space and time framework for accumulations to form. Conversely, Gas shale acts as the source rock, reservoir and trap simultaneously. In other words, gas shale is a source rock with a significant amount of residual gas or a gas-charged, self-sourced, fine-grained (dominantly<4 um), organic-rich (Total Organic Carbon or TOC >0.5) reservoir and with permeabilities in the range of 0.01 to 0.0001 mD. Shale gas often refers to the gas stored in the gas shale. This unconventional resource is less concentrated but more prevalent than conventional gas resources. The main parameters evaluating the prospect of shale are the initial content of organic matter (TOC) and the thermal maturity (7). In other words, thermal maturity is how much heat the rock has been subjected to in order to transform kerogen into hydrocarbon. This is typically measured by the process of pyrolysis or by measuring vitrinite reflectors. (6)

Another way to define shale gas is by saying it's the natural gas stored in organic rich fine-grained reservoirs in the form of both adsorbed gas and free gas. The adsorbed gas is stored on the surface of the organic compounds while the free gas is stored in the matric and fracture porosity. This adsorbed gas is liberated of the rocks' surface as pressure declines in the reservoir; this is often linked to the free gas production within the fracture network. Quartz-rich shale gas plays are dominated by free gas production while organic material and clay minerals are dominated by adsorbed gas production (8). It is worth noting that shale gas is a dry gas composed primarily of methane (more than 90%) with some fractions of nitrogen, ethane, propane, carbon dioxide and water. However, some shale gas reservoirs (Eagle Ford Shale) also contain wet gas and gas condensate (9).

2.1.2 Shale Oil

Shale oil is produced from oil shale rock fragments by pyrolysis, hydrogenation, or thermal dissolution. These processes alter the kerogen in the rock (organic matter) into oil and gas resulting in an oil that can be used as a fuel or refined by adding hydrogen and removing impurities. The refined products and crude oil derived products can be used for the same purposes. (10)

2.2 Drilling a Fractured Horizontal Shale Gas well

Shale gas can be produced from shale formation by horizontal drilling followed by hydraulic fracturing. The combination of both allows for the recovery and production of natural gas contained inside the low-permeability formations in an economical way. This however depends on a large and sustained flow rate backed up by favorable gas market prices.

Shale gas reservoirs are vertically very thin. Instead they extend horizontally for multiple kilometers squared. Therefore, horizontal drilling is favorable in the case of shale reservoirs. The horizontal well gives access to a much larger portion of the reservoir (up to 2 or more kilometers) while vertical wells provide a much smaller contact. Drilling begins with a vertical well that starts deviating a few meters above the reservoir until it is fully horizontal, and the planned length is reached as shown in the figure below. Multiple horizontal wells extend from the single vertical well pad at times even reaching 40 wells per pad.

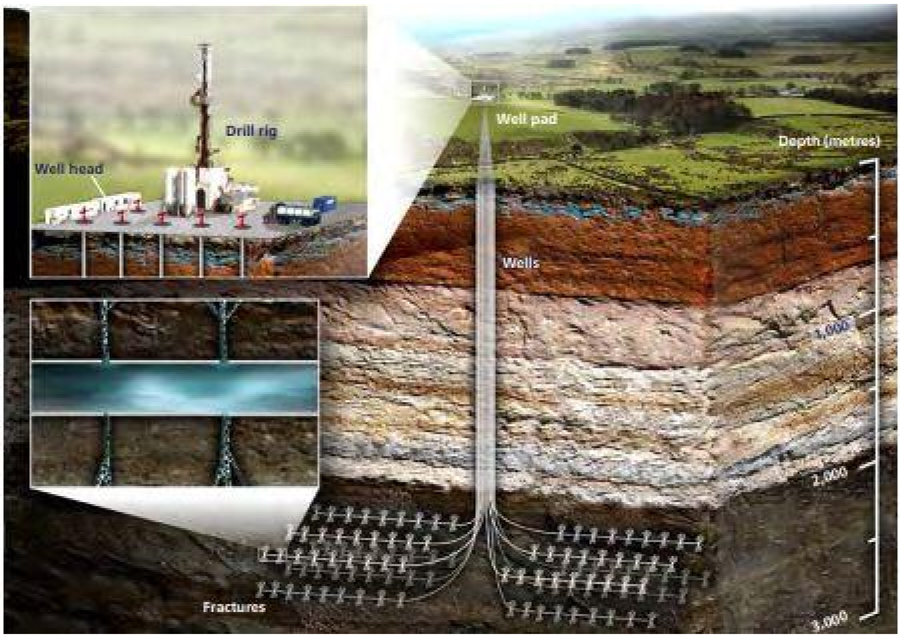

Figure 6: Example of horizontal drilling and hydraulic fracturing from a multi-well pad. (4)

Horizontal wells are not only useful for reaching a larger reservoir area, it also allows contacting surfaces which would not have been accessible by vertical drilling in instances where the reservoir is located in a populated area or a park. The well can be drilled just outside the populated area and then deviated horizontally to reach the required locations. Horizontal wells can cost up to three times as much as vertical wells. However, the enhancement in recovery covers that cost and when combined with fracking produces very high recovery factors.

In order to maximize the production potential of the well, the shale formation is hydraulically fractured. This is necessary due to the very low permeability of the shale rocks. Fracking leads to an increase in the flow rate from the reservoirs and decrease in the pressure drop around the well. In the case of shale gas reservoirs, fracking is done in such a way that connects the horizontal well to the full vertical extent of the reservoir thus reaching the farthest parts of the reservoirs and increasing production. In cases where natural fractures are also present, the induced hydraulic fractures connect the natural ones to the wellbore also allowing for a larger drainage area.

The low permeability of shale reservoirs provides resistance to fluid flow. This is why shale formations are excellent candidates for fracking. Another parameter that is critical to hydraulic fracturing is the in-situ stress distribution. A favorable in-situ stress barrier is one that minimizes the vertical height growth of the reservoir with changes in the pressure.

Today, slick water is used as a fracturing fluid for shale reservoirs in addition to low proppant concentrations to stimulate the low permeability of the reservoirs (11).

The usage of the frac-method mentioned above is successful due to the necessity of cost-cutting, less formation damage and efficient cleanup of the reservoir and the creation of more complex fractures (12).

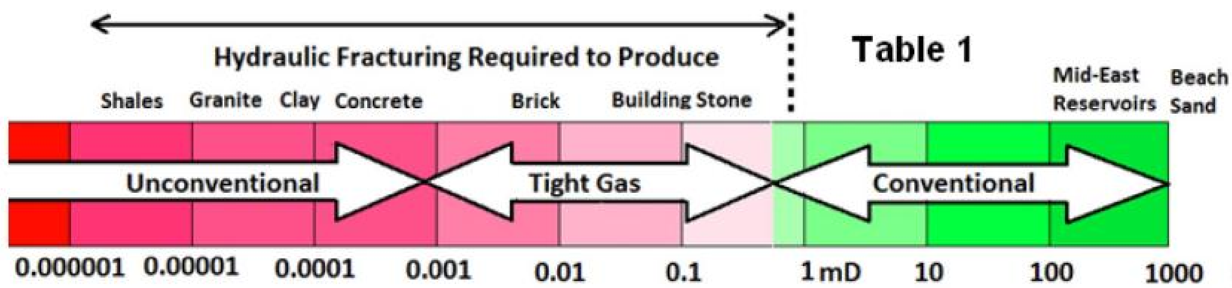

Figure 7 : Permeability range for producing formations and where fracturing is required (12)

The hydraulic fracture is created by pumping a huge amount of fluid into the rock formation (wellbore) exceeding the fracture gradient (downhole pressure) of the rock and consequently cracking the rocks and reopening sealed natural fractures. Though the fractures’ horizontal growth can be controlled to a certain extent, vertical growth can extend to hundreds of feet above the pay zone and fracturing fluid can be lost to the surrounding permeable formations. The geometry of the fractures is influenced by the in-situ stresses, the rock geo-mechanical properties, the fracturing fluid used and local heterogeneities (13).

The in-situ stresses control many parameters of the hydraulic fractures like the width, direction of propagation and the height growth. Moreover, the closure pressure, instantaneous shut-in pressure and fracture propagation pressure are influenced by the minimum in-situ stress.

The fracturing fluid injection rate greatly impacts the geometries of the fractures. A high injection rate would create more planar hydraulic fractures while a slower one would reopen the natural fracture system. According to seismic data a bigger stimulated reservoir volume is created when there are more intersections between the induced hydraulic fractures and the natural fractures already present in the reservoir.

Chapter 3: Methodology

3.1 Shale Gas Production and Physical Mechanisms

This paragraph discusses some important mechanisms that may control shale gas production and decline curves. These factors and their coupled effects on the overall horizontal well performance will be the focus of this thesis.

3.1.1 Gas Adsorption

In shale gas reservoirs, gas can be stored as compressed fluid inside the pores or it can be absorbed by the solid matrix. In other words, the accumulated gas on the grains of the reservoir rock or on the organic particles due to the increased pressure is called adsorbed gas. On the other hand, free or pore gas (interstitial gas) is stored in the pore space of the reservoir rock. The combination of the two mentioned before allows the calculation of the total gas in place for the reservoir. The gas adsorption in a shale gas system is mainly controlled by the presence of organic matter and the gas adsorption capacity depends on the TOC (Total Organic Carbon), organic matter type, thermal maturity and clay minerals. Generally, a higher TOC content implies a greater gas adsorption capacity. In addition, the high amount of nanopores lead to a significantly small porosity in shale formations, which increases the gas adsorption surface area considerably. The amount of adsorbed gas varies from 35-58% (Barnett Shale, USA) up to 60-85% (Lewis Shale, USA) of total gas initial in place. The figure 7 shows laboratory measurements of gas adsorption capacity from a shale sample at different temperatures. As we can observe, the reservoir pressure must be adequately low to liberate the adsorbed gas. For organically rich shales, the ultimately recoverable amount of gas is largely a function of the adsorbed gas that can be released (desorbed). Understanding the effects that initial adsorption, and moreover, desorption has on gas production and decline trend will increase the effectiveness of reservoir management and economic evaluations.

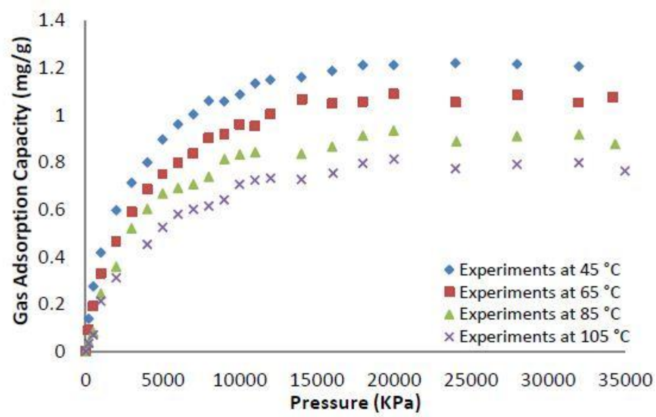

Figure 8:Gas adsorption capacity from Jiashiba Shale sample at different temperatures (ref)

When a shale gas well starts production, the adsorbed gas layer begins liberating and rock compaction occurs. The release of the adsorbed gas helps compensate for the pressure loss in the stimulated reservoir volume during the initial stages of production. Consequently, more gas can be produced for the same pressure level.

3.1.2 Klinkenberg Effect and Langmuir Model

Klinkenberg discovered in 1941 that the permeability to gas is higher than that to water and called this occurrence as slip flow (gas slippage) between the solid walls and the gas molecules. The gas molecules collide each other as well as the pore-walls and when the mean free path get close to the pore radius more collisions occur, and an additional flux called slip flow enhances the flow rate. The following formula explains how the permeability K of gas differs from that of a liquid.

$$K_g = K_L(1 + \frac{b}{p}) \ldots\ldots\ldots\ldots\ldots\ldots\ldots\ldots\ldots\ldots \text{(eq 1)}$$

Where p is the pore pressure and b also known as the klinkenberg slip factor is determined as a function of the temperature, mean free path and the pore radius.

The Langmuir model on the other hand is used to describe the adsorption of a gas by assuming that it behaves as an ideal gas at isothermal conditions. This assumption correlates the adsorbed gas's pressure to the volume adsorbed onto the solid rock.

These two parameters' incorporation into a reservoirs model are crucial for proper simulation of a gas reservoir in general and even more important for shale gas reservoirs characterized by the extremely low permeability and porosity of the formations.

3.1.3 Matrix Apparent Permeability and its Evolution

Darcy's equation, which models pressure-driven viscous flow, works properly for reservoirs where continuum theory holds, and fluid velocity can be assumed to be zero at the pore wall. However, in shale reservoirs which have pores in the range of nanometers, fluid continuum theory breaks down and gas molecules follow a random route while still preserving a general flow direction governed by the pressure gradient. When comparing shale with sand, the much higher permeability of sand allows for an easier flow of fluid through the pores. Instead of having zero velocity, molecules strike against the pore walls and tend to slip. To propose corrections for non-Darcy flow over different flow regions in very small pore space, several authors have measured these effects by altering the slippage factor or determining the apparent permeability as a function of Knudsen number.

Multiple theoretical and empirical models have been developed for apparent permeability enhancement in nanopore matrixes, to account for the effects of non-Darcy flow/gas-slippage behavior, they disregard the changes in pore structure geometry induced by stress variations and the release of the adsorption gas layer during production. With constant decreasing pore pressure and increasing effective stress, the formation's structure will be affected. Wang and Marongiu-Porcu indicated in their work that despite rock compaction, the apparent permeability in shale matrix increases during production due to the combined effects of non-Darcy flow/gas-slippage and release of the adsorption gas layer (14). The evolution of matrix permeability as reservoir pore pressure declines can also make a difference in determining gas production rate.

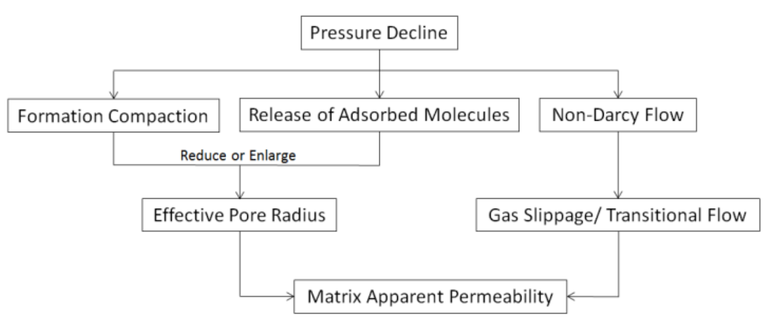

Figure 9:Mechanisms that alter shale matrix apparent permeability during production (14)

3.2 Reference Case and Reservoir Model Description

In this simulation study, a field-scale shale gas reservoir model was built using a commercial reservoir simulator (Rubis 5.2) by Kappa Engineering. The reservoir is 3,400ft in length, 2020ft in width and 100ft in thickness. A horizontal well with a lateral length of 2400ft was considered. It was completed using 25 hydraulic fractures along the horizontal wellbore with a fracture conductivity of 100 mD.ft. Many cases were taken into consideration with the base case assuming a simple fracture geometry where hydraulic fractures are orthogonal/planar. In addition, to account for the complex transport mechanisms of shale gas, both gas desorption and gas slippage were considered in this model. Regarding gas desorption, the Langmuir model was considered. Regarding gas slippage, the Klinkenberg effect was considered with a reference pressure of 500 psi. Following that is a tabulated summary of the basic reservoir and fracture parameters considered in this reservoir model (15)

Parameter	Value	Unit
Model Dimensions [LxWxH]	3400x2020x100	Ft
Initial reservoir pressure	4,000	Psi
Reservoir temperature	130	F
Matrix porosity	6	%
Matrix permeability	0.0001	mD
Rock density	2.5	g/cm3
Rock compressibility	3 × 10^-6	1/psi
Langmuir pressure	1,300	Psi
Langmuir volume	140	Scf/ton
Klinkenberg reference pressure	500	Psi
Fracture conductivity	100	mD.ft
Fracture height	100	Ft
Fracture aperture/width	0.01	Ft
Base case fracture half length	510	Ft
Minimum bottom-hole pressure	500	psi

Table 1: Basic reservoir parameters (15)

The base case consists of 25 planar fractures (90° fracture angle from wellbore). These fractures had a uniform distribution with a fracture half-length of 510ft and a fracture aperture of 0.01 ft. Figure 9 shows the 2D map of the base case.

3.3 Case studies

For this study, more than 30 simulation cases were made using the commercial simulator Rubis 5.2 by Kappa Engineering. The cases were assumed all simple but with varying fracture angles to analyze the effect of the angle on well performance. Further cases saw a change in the fractures' half-length and later a change in the number of fractures by doubling then dividing by two over the same well length was done.

The base case was explained in the previous subchapter. A brief summary of each further case will be written below followed by 2D maps of each case is displayed, showing the reservoir, the well and the fractures' geometries.

It is worth noting that the first 20 cases assumed single phase gas flow and the analysis was made on its geometrical parameters.

The following table summarizes the different fracture geometry of each case

	Number of Fractures	**Angle of Fractures**	**Half-length (ft)**	**Total Length (ft)**
Case 1	25	90	510	25500
Case 2	25	70	510	25500
Case 3	25	50	510	25500
Case 4	25	30	510	25500
Case 5	25	90	510/390	22620
Case 6	25	70	510/390	22620
Case 7	25	50	510/390	22620
Case 8	25	30	510/390	22620
Case 9	25	90	510/390	24540
Case 10	25	70	510/390	24540
Case 11	25	50	510/390	24540
Case 12	25	30	510/390	24540

Case 13	12	90	510	12240
Case 14	50	90	510	51000
Case 15	50	90	255	25500
Case 16	25	90	255	12750
Case 17	12	90	255	6120
Case 18	12	50	255	6120
Case 19	25	50	255	12750
Case 20	50	50	255	25500

Table 2: Fracture Parameters of each case

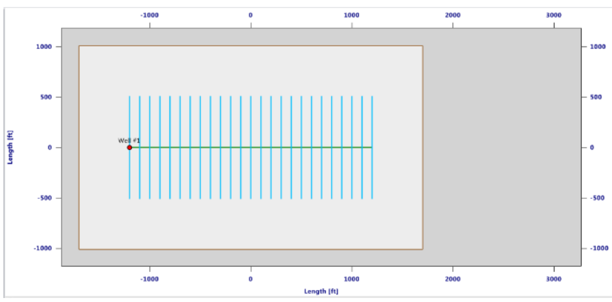

Figure 10: 2D map of the base Case

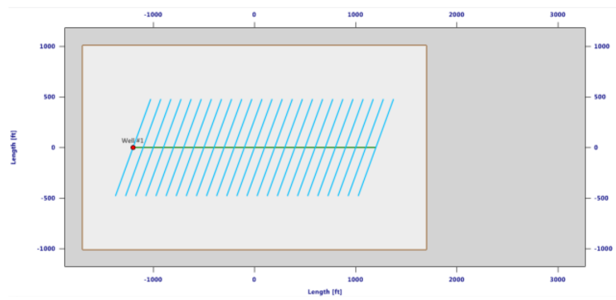

Figure 11: 2D map of case 2

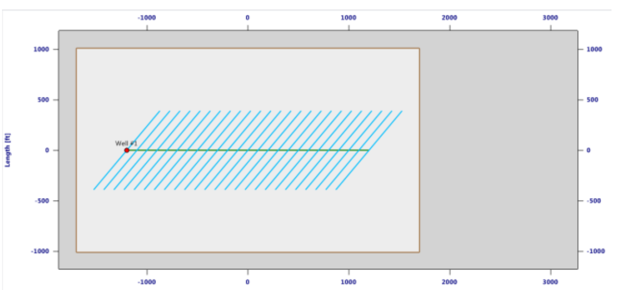

Figure 12: 2D map of case 3

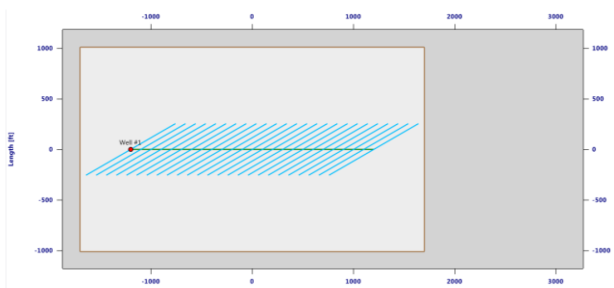

Figure 13: 2D map of case 4

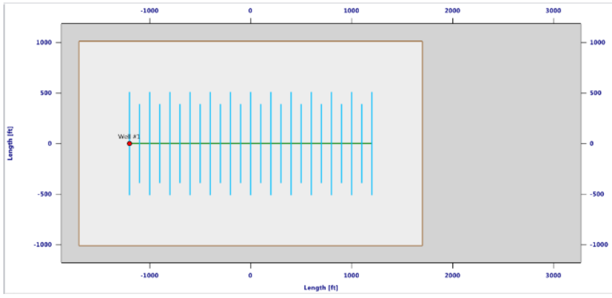

Figure 14: 2D map of case 5

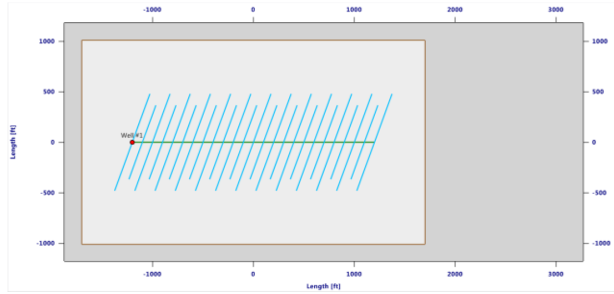

Figure 15: 2D map of case 6

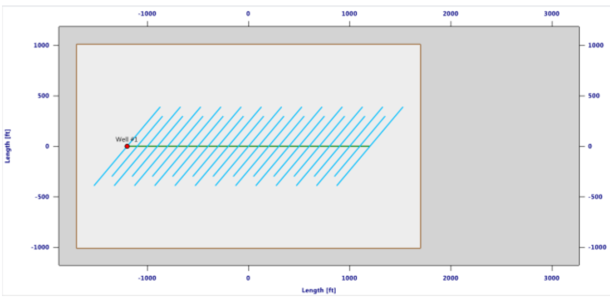

Figure 16: 2D map of case 7

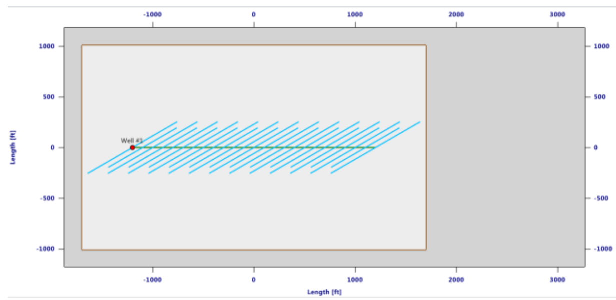

Figure 17: 2D map of case 8

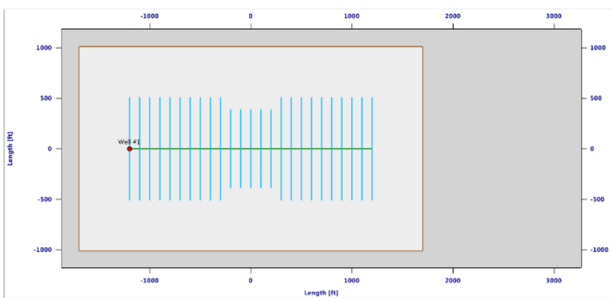

Figure 18: 2D map for case 9

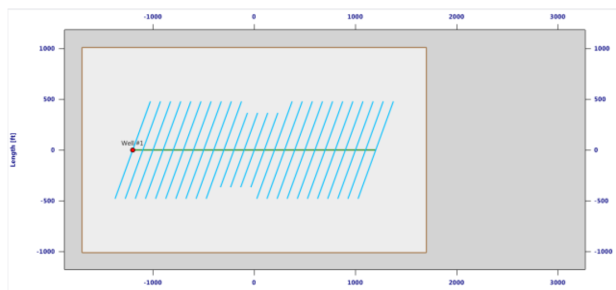

Figure 19: 2D map for case 10

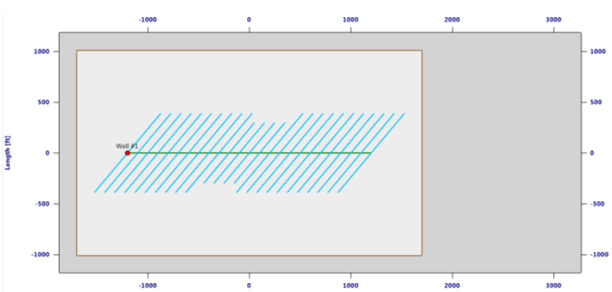

Figure 20: 2D map for case 11

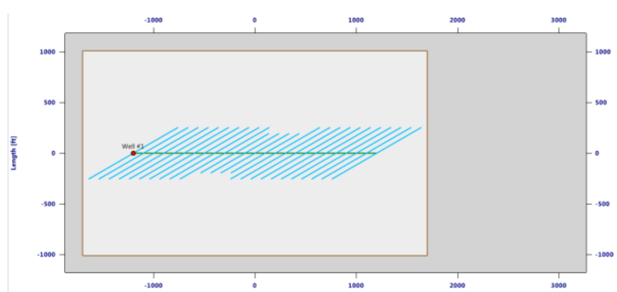

Figure 21: 2D map for case 12

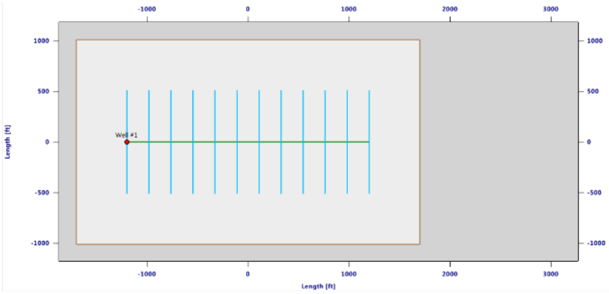

Figure 22: 2D map of case 13

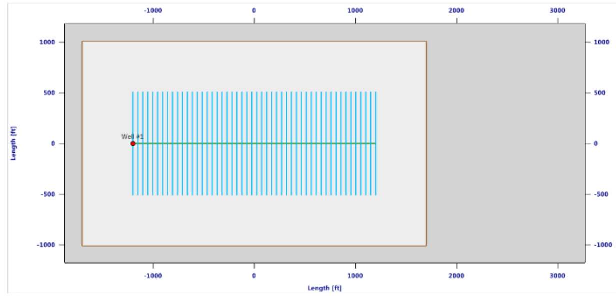

Figure 23: 2D map of case 14

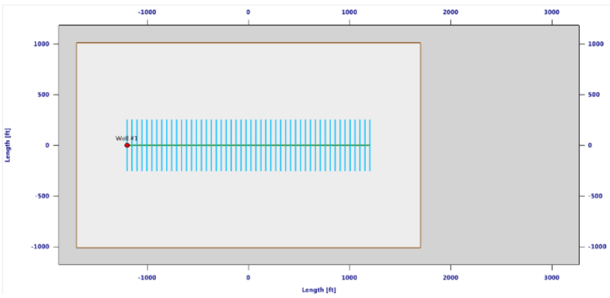

Figure 24: 2D map of case 15

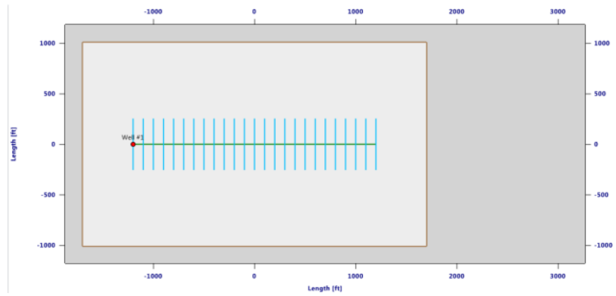

Figure 25: 2D map of case 16

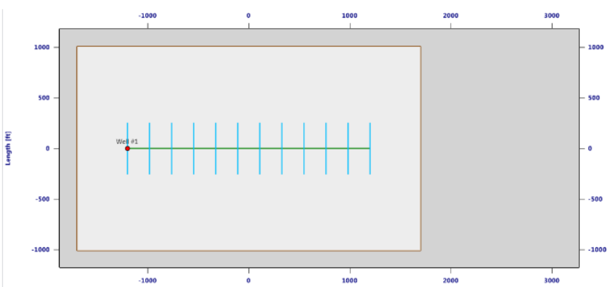

Figure 26: 2D map of case 17

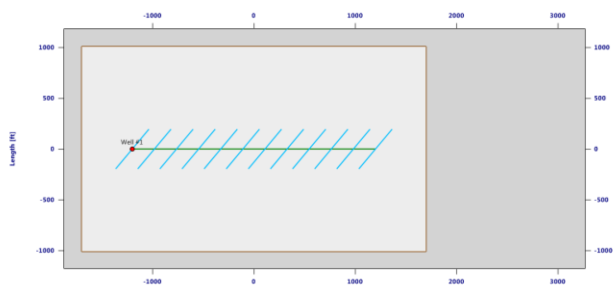

Figure 27: 2D map of case 18

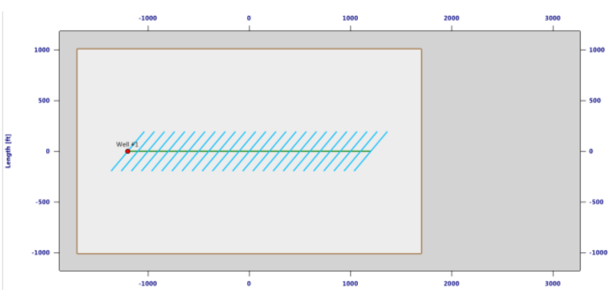

Figure 28: 2D map of case 19

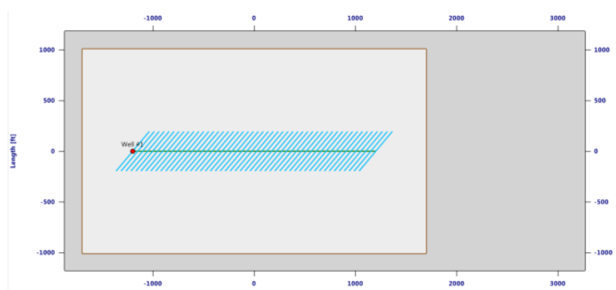

Figure 29: 2D map of case 20

Chapter 4: Results and Analysis

4.1 Well Performance

The mentioned cases were used to quantify the effect of changing fracture angles and half lengths on the shale gas well performance.

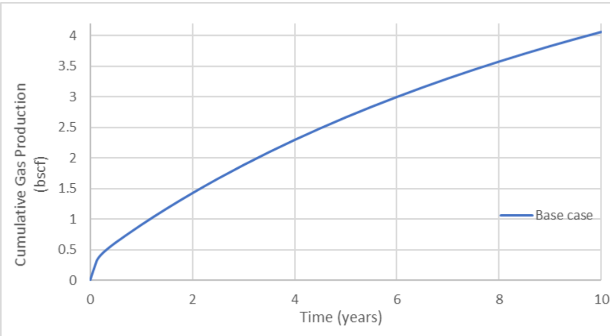

Figure 30: Cumulative Gas Production for the Base Case

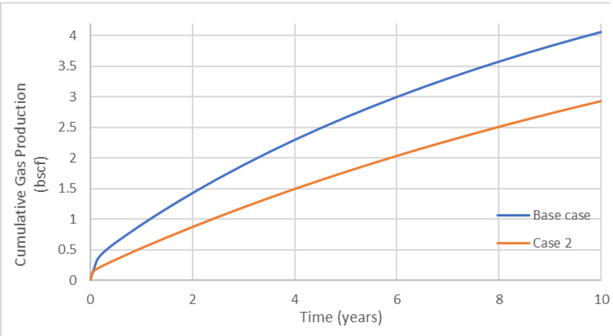

Figure 31:Comparison of Cumulative Gas Production for Base Case1 and Case 2

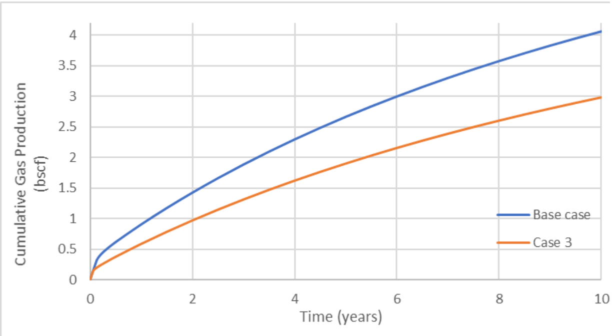

Figure 32: Comparison of Cumulative Gas Production for Case 1 and Case 3

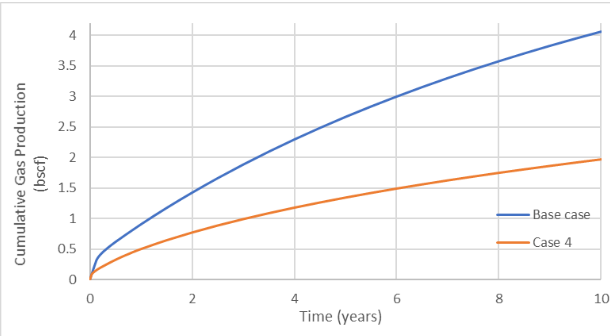

Figure 33: Comparison of Cumulative Gas Production for Case 1 and Case 4

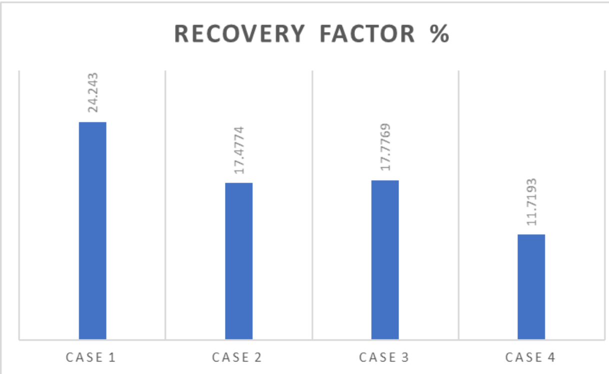

Figure 34: Recovery Factor for the First 4 Cases

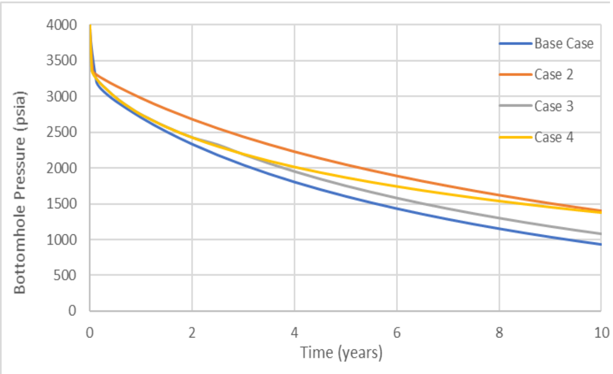

Figure 35: Pressure Decline for the First 4 Cases

The first four cases discuss the effect of the change in the fracture angle on the overall well performance. The figures above display the 10-year simulated cumulative gas production for a reservoir with constant parameters, a horizontal well with non-changing variables except for the fracture angle. The results are tabulated below. With the percentage change from the first planar case shown.

	Base Case	Case 2	Case 3	Case 4
Cumulative Gas Production at 10 Years (bscf)	4.06177	2.93178	2.98204	1.96588
% Change in Cumulative Gas Production at 10 years from the Planar (base case)		-27.8%	-26.6%	-51.6%

Table 3: Summary of Cumulative Gas Production (bscf) and the percentage change from the planar (base) case at the end of the 10 years for the different hydraulic fractures' cases

As can be seen from the figures and tables above, the base case had the best recovery out of all cases, while the second two cases behaved in a similar way with about 27% decrease in the amount of gas recovered from the reservoir. As expected, the base case had the highest pressure depletion. However, the other cases had a depletion profile that correlates between the cumulative production and the fractures' proximity to the boundaries.

The next 4 cases presented consider not only the effect of changing the angle, but also the effect of alternating the fractures' half-length 510ft at a time then 390ft after.

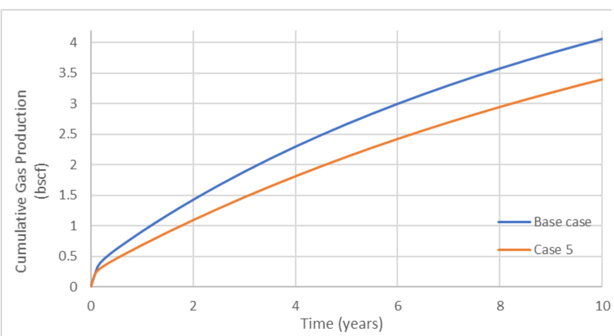

Figure 36: Comparison of Cumulative Gas Production for Base Case and Case 5

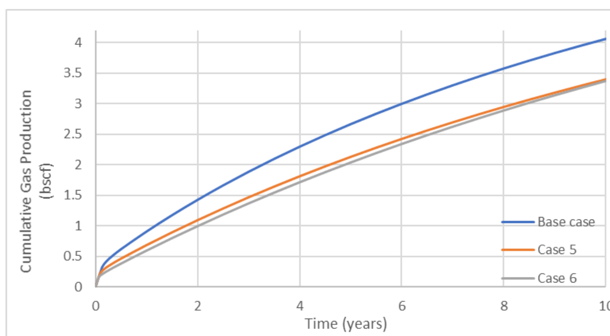

Figure 37: Comparison of Cumulative Gas Production for Case 1, Case 5 and Case 6

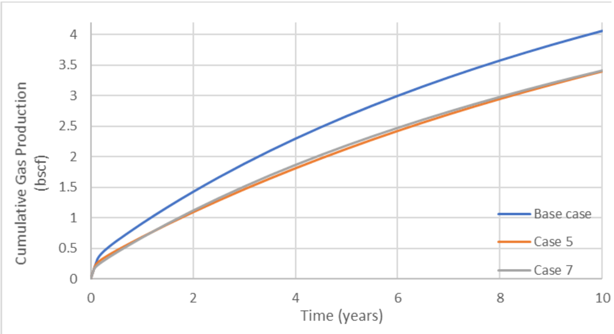

Figure 38: Comparison of Cumulative Gas Production for Case 1, Case 5 and Case 7

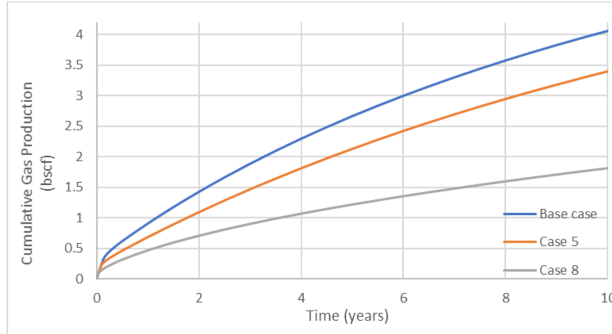

Figure 39: Comparison of Cumulative Gas Production for Case 1, Case 5 and Case 8

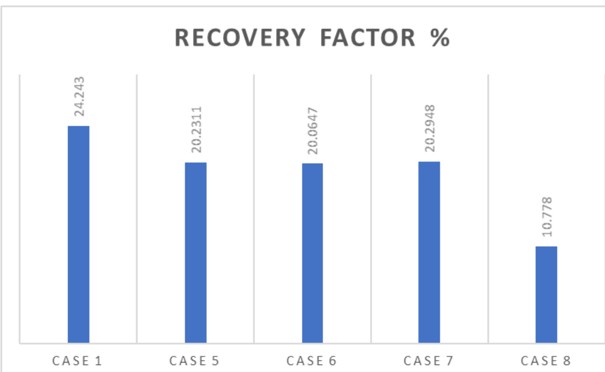

Figure 40: Recovery Factors for the 2nd Group of Cases

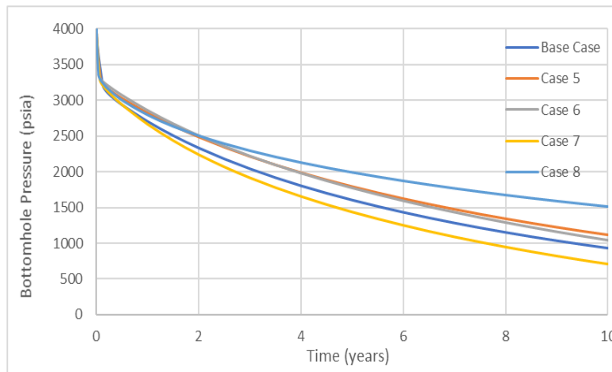

Figure 41: Pressure Decline for the 2nd Group of Cases

The second 4 cases, which demonstrate a non-realistic fracture geometry, show the effect of the presence of smaller fractures between each other fracture. The main fracture half-length was kept at 510ft, while each other fracture was made at 390ft. The results tabulated below show not only the cumulative gas production and percentage change comparing to the base case of the 4, but also comparing the angles to one another between the first group of four cases and the second.

	Case 5	Case 6	Case 7	Case 8
Cumulative Gas Production at 10 Years (bscf)	3.3942	3.3653	3.40388	1.80771
% Change in Cumulative Gas Production at 10 years from Case 5		-0.85%	0.28%	-46.74%
% Change in Cumulative Gas Production at 10 years from Base Case	-16%	-17%	-16%	-55%

Table 4:Summary of Cumulative Gas Production (bscf), the percentage change from the planar (base) case at the end of the 10 years and the percentage change from case5

As can be seen above, cases 5,6 and 7 behaved in a similar manner producing the same amount of gas in the 10-year simulation period. However, the recoverable gas reduced by about 16% from the base case. On the other hand, case 8 saw a drastic reduction in gas recovery (46% from similar cases and 58% from the base case). Moreover, at the end of the simulation period case 8 had the highest reservoir pressure which means more gas can be recovered with further production.

Another group of cases was simulated. This time, the 4 mid fractures had a half-length on 390ft while the remaining had a half-length of 510ft.

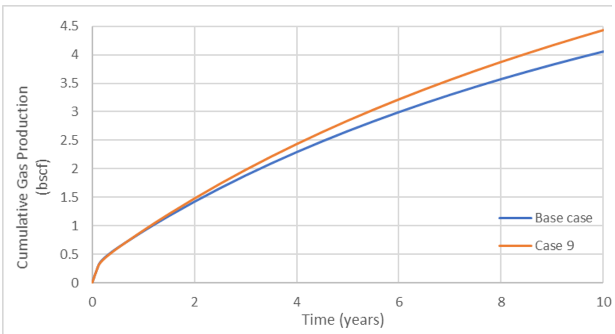

Figure 42: Comparison of Cumulative Gas Production for Case 1 and Case 9

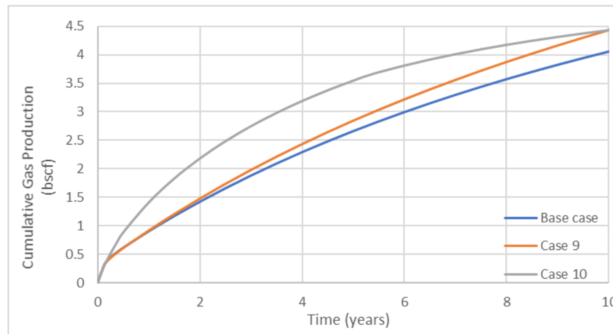

Figure 43: Comparison of Cumulative Gas Production for Case 1, Case 9 and Case 10

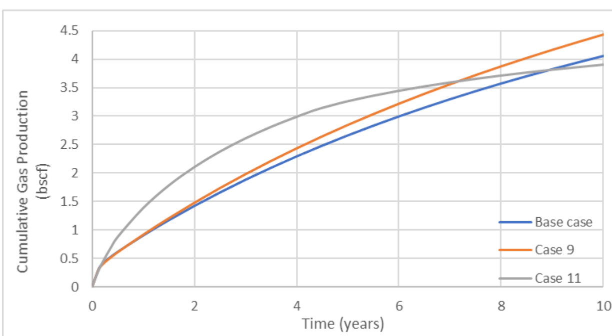

Figure 44: Comparison of Cumulative Gas Production for Case 1, Case 9 and Case 11

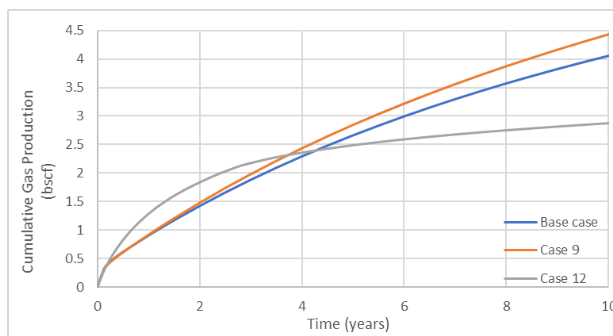

Figure 45: Comparison of Cumulative Gas Production for Case 1, Case 9 and Case 12

As seen above, case 9 produced slightly higher gas over the simulation period with a flow pattern similar to that of the base case. Case 10 production value was no different than case 9 but a higher cumulative production was noted during the first few years of the simulation. The remaining two cases also had a higher cumulative production during the first few years. However, the final recovery varied with less recovery the smaller the angle became. A better explanation for this can be made when the pressure decline is compared. As can be seen cases 10,11 and 12 had a higher pressure decline during the early years of production. The smaller the angle, the sharper the decline slope until the drawdown value of 500psi is reached; after which gad flow continues at that pressure.

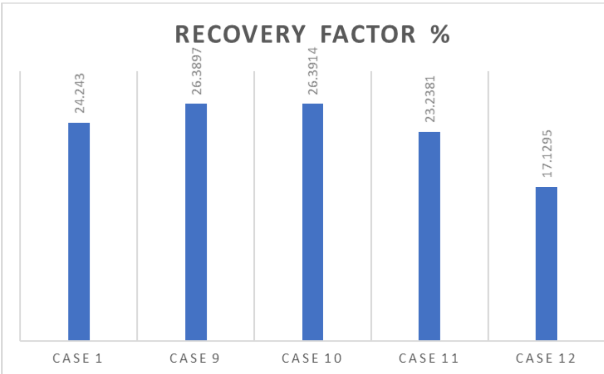

Figure 46: Recovery Factors of 3rd Group of Cases

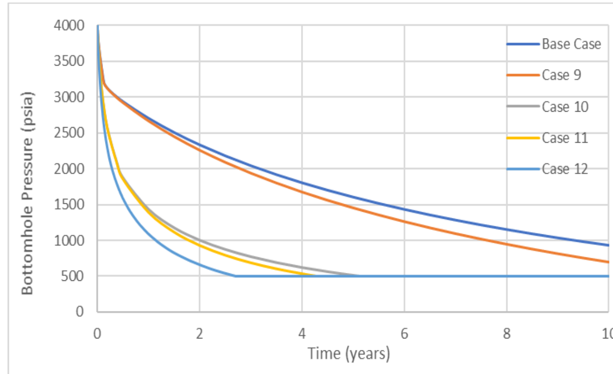

Figure 47: Pressure Decline for 3rd Group of Cases

	Case 9	Case 10	Case 11	Case 12
Cumulative Gas Production at 10 Years (bscf)	4.42778	4.42686	3.89792	2.87329
% Change in Cumulative Gas Production at 10 years from case 9		-0.02%	-11.96%	-35.10%
% Change in Cumulative Gas Production at 10 years from Base case	9%	8%	-4%	-29%

Table 5:Summary of Cumulative Gas Production (bscf) and the percentage change from the planar case at the end of the 10 years for the different hydraulic fractures' cases

The last 8 cases take only two angles (90 and 50) and compares how the number of fractures for the same well length and the fractures' half-lengths affect the performance.

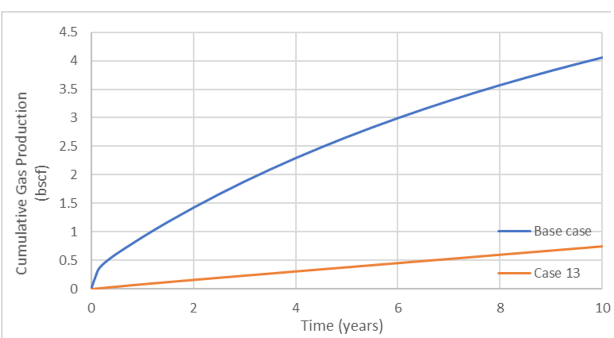

Figure 48: Comparison of Cumulative Gas Production for Case 1 and Case 13

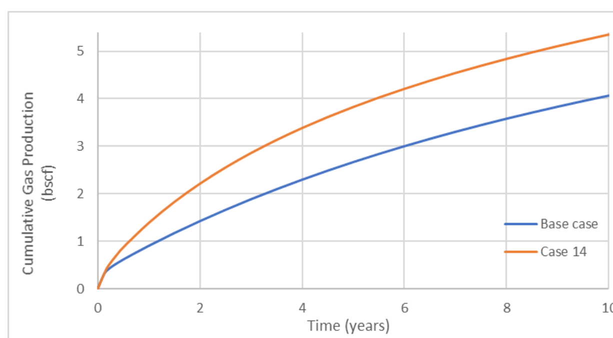

Figure 49: Comparison of Cumulative Gas Production for Case 1 and Case 14

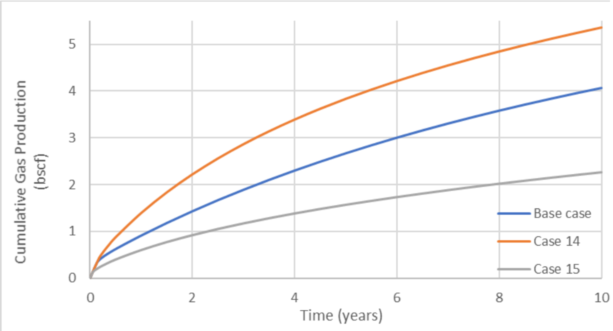

Figure 50: Comparison of Cumulative Gas Production for Case 1, Case 14 and Case 15

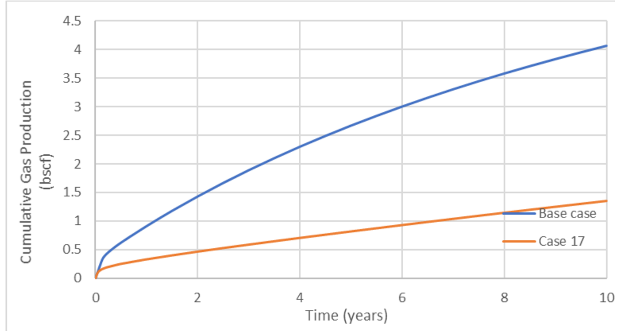

Figure 51: Comparison of Cumulative Gas Production for Case 1 and Case 16

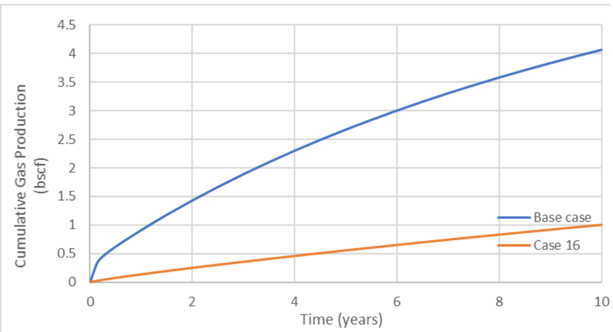

Figure 52: Comparison of Cumulative Gas Production for Case 1 and Case 17

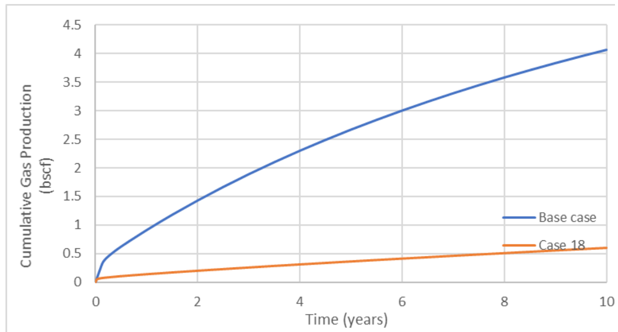

Figure 53: Comparison of Cumulative Gas Production for Case 1 and Case 18

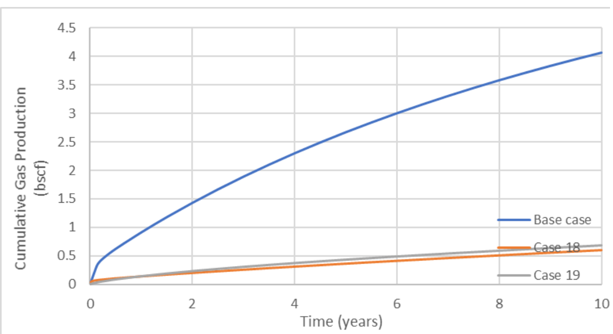

Figure 54: Comparison of Cumulative Gas Production for Case 1, Case 18 and Case 19

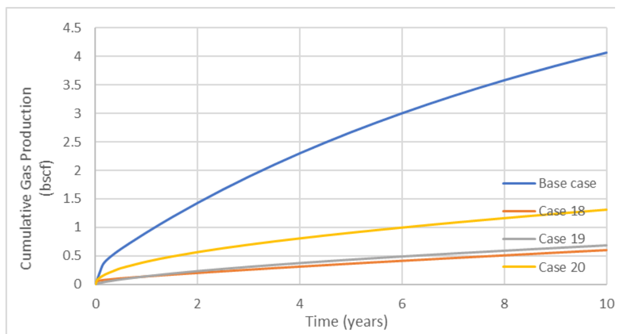

Figure 55: Comparison of Cumulative Gas Production for Case 1, Case 18, Case 19 and Case 20

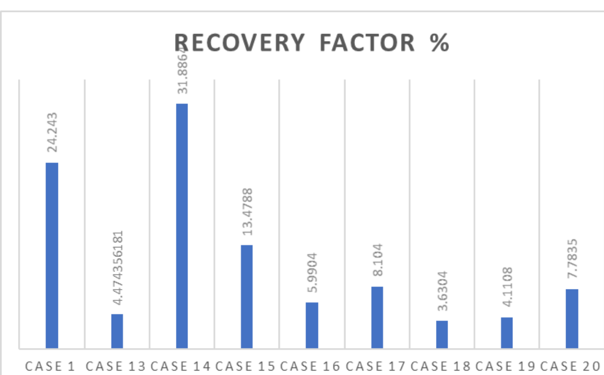

Figure 56: Recovery Factors of the 4th Group of Cases

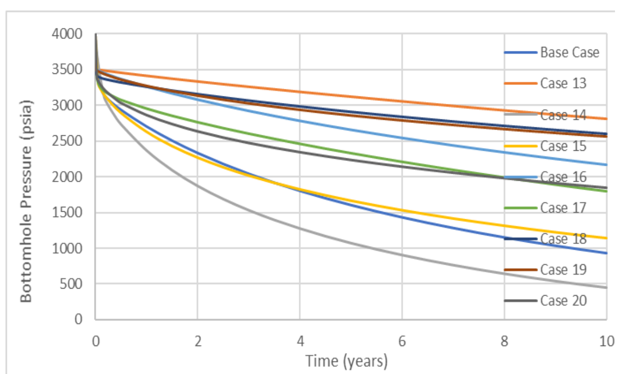

Figure 57: Pressure Decline for the 4th Group of Cases

The graphs above show clearly how much the number of fractures can influence the overall production. That is also highlighted when the fractures' half-length is reduced to half as that also drastically reduces the well performance. The table below provides a summary of the results highlighting the production at the end of the 10-year period and the percentage change for each relative case.

	Case15	**Case16**	**Case17**	**Case18**	**Case19**	**Case20**
Cumulative Gas Production at 10 Years (bscf)	2.26	1.358	1.00419	0.608	0.689	1.305
% Change in Cumulative Gas Production after doubling number of fractures	66.42%					89.4%
% Change in Cumulative Gas Production after halving number of fractures			-26%	-11.7%		
% Change in Cumulative Gas Production for angle change with same number of fractures				-39.4%	-49%	-42.2%

Table 6: Summary of Cumulative Gas Production (bscf) and the percentage change from a base case at the end of the 10 years for the different hydraulic fractures' cases

Halfling the number of fractures has a huge effect on production with only 5% RF (case 13) as opposed to 24% for the base case, while doubling it recovered 31% (case 14) of the reservoir. This effect is heightened for larger fracture half-lengths. On the other hand, when Xf was reduced to half (cases 15,16 and 17), the RF was substantially higher for 50 natural fractures with a 66% increase from case 16 (25 natural fractures) while case 17 (12 natural fractures) had a 26% decrease only.

Another parameter investigated, was the fracture angle for a lower Xf. It was observed that the angle made a high difference when the number of fractures was also high (larger SRV) while for lower fracture numbers, cumulative production was similar.

The pressure decline curves show that the more fractures we have, the higher the decrease in reservoir pressure is. Moreover, decreasing the fractures' half-length resulted in a smaller pressure decline. In the end, all decline curves has a somewhat similar (parallel) decline slope with the end value varying depending on how big the SRV (drainage area) is.

4.2 Pressure Distribution

The pressure distribution in the reservoir was recorded at every timestep. In the figures below, the pressure distribution is displayed for each case at time 0, after 6 years and after 10 years.

As expected, due to the very low permeability value of the matrix, the pressure in the volume not affect by matrix remain unaltered and equal to the initial vale

Base Case

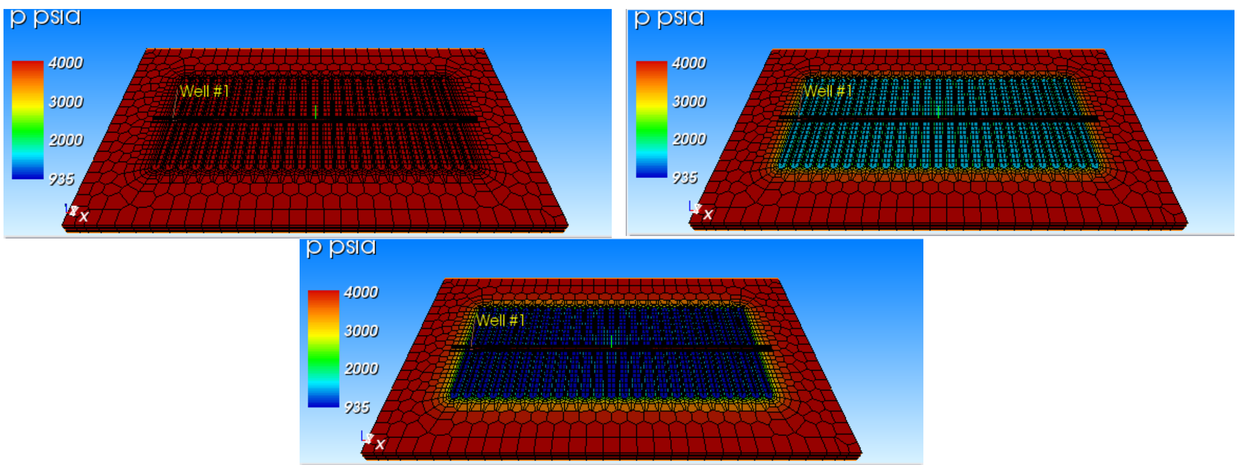

Figure 58:3D pressure distribution maps before production, at time 6 years and at 10 years for base case

Case 2

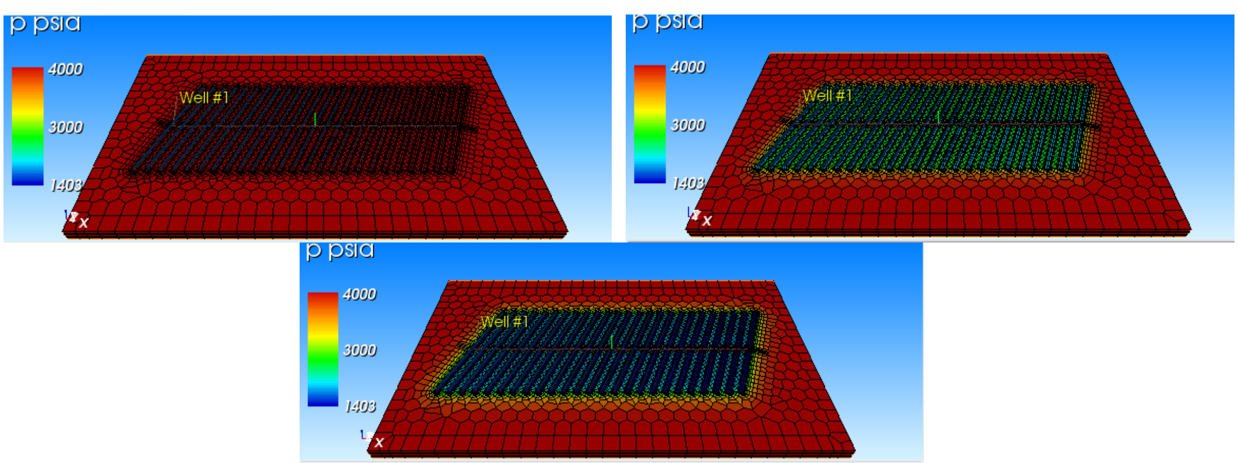

Figure 59: 3D pressure distribution maps before production, at time 6 years and at 10 years for case 2

Case 3

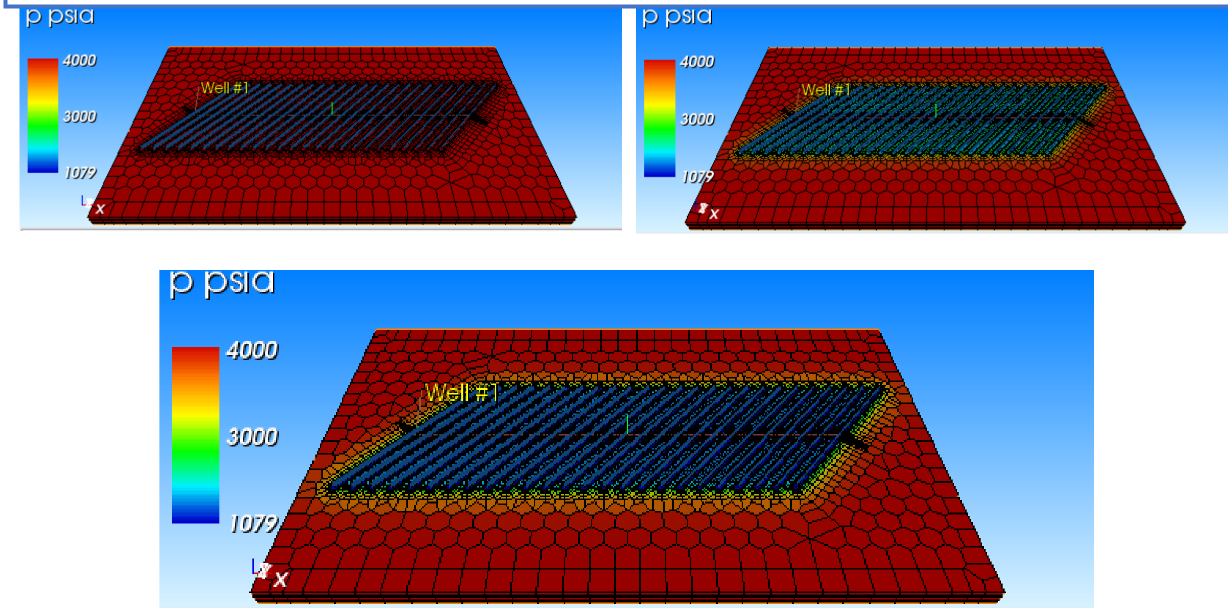

Figure 60:3D pressure distribution maps before production, at time 6 years and at end of production (10 years) for case 3

Case 4

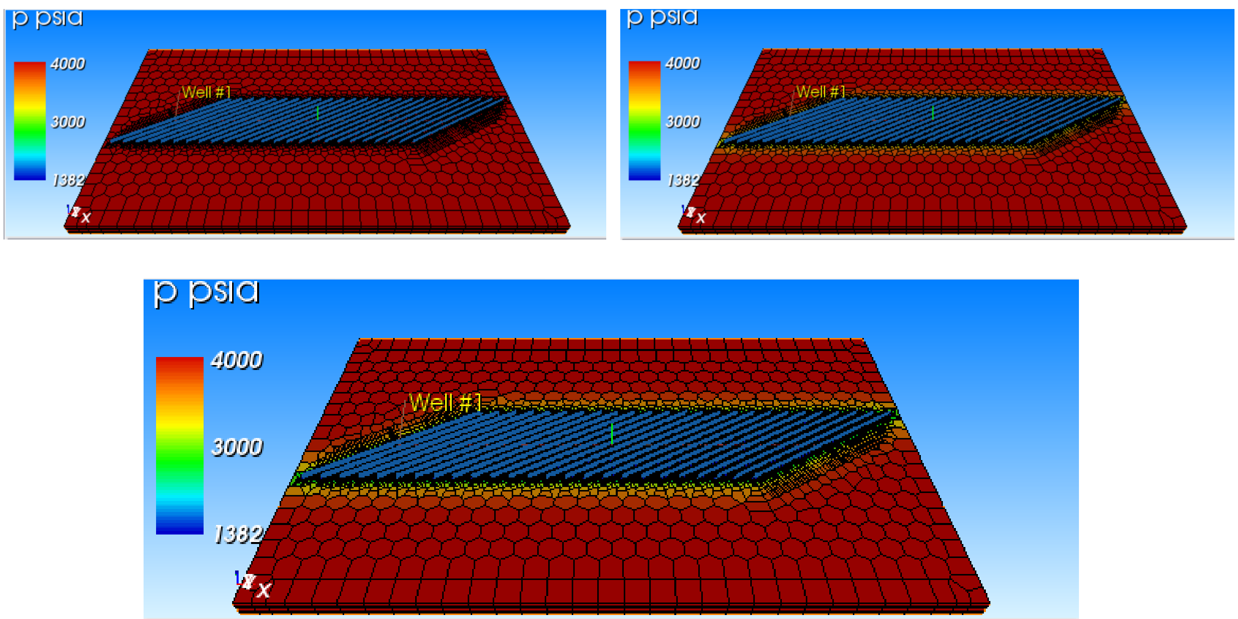

Figure 61: 3D pressure distribution maps before production, at time 6 years and at end of production (10 years) for case 4

Case 5

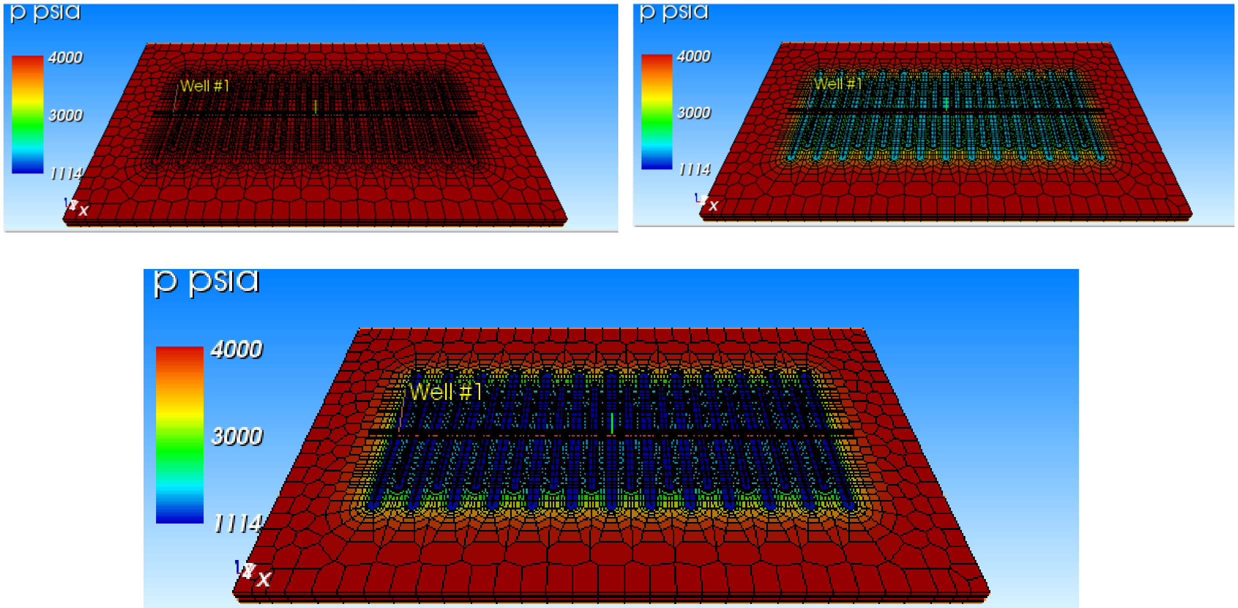

Figure 62: 3D pressure distribution maps before production, at time 6 years and at end of production (10 years) for case 5

Case 6

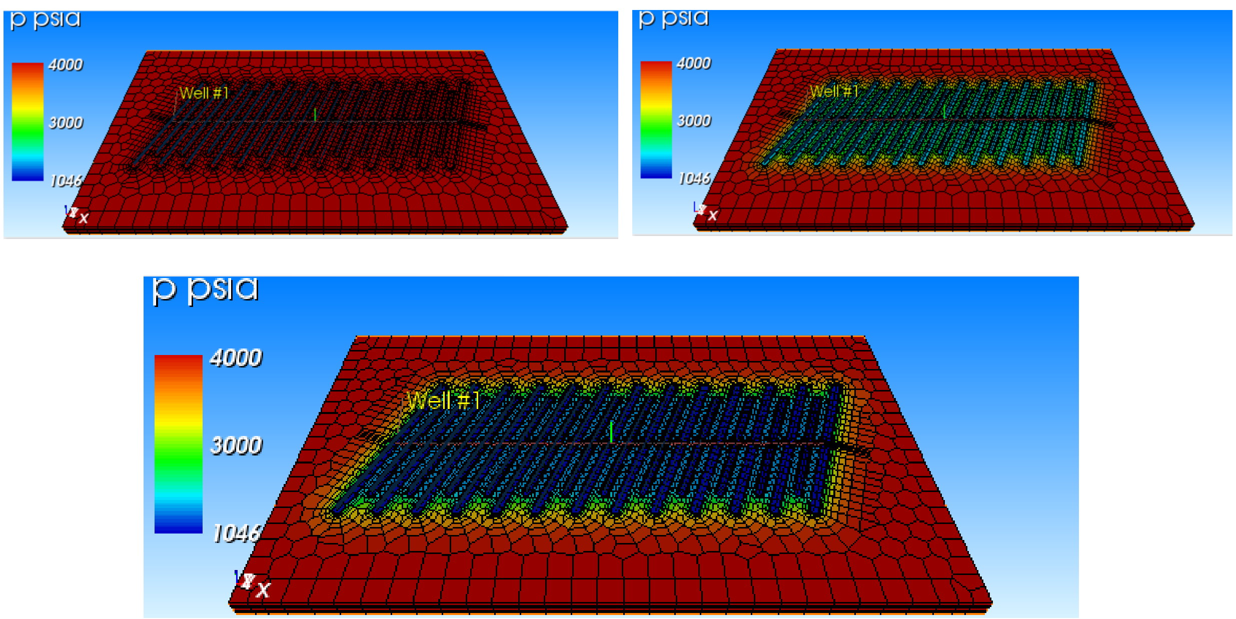

Figure 63: 3D pressure distribution maps before production, at time 6 years and at end of production (10 years) for case 6

Case 7

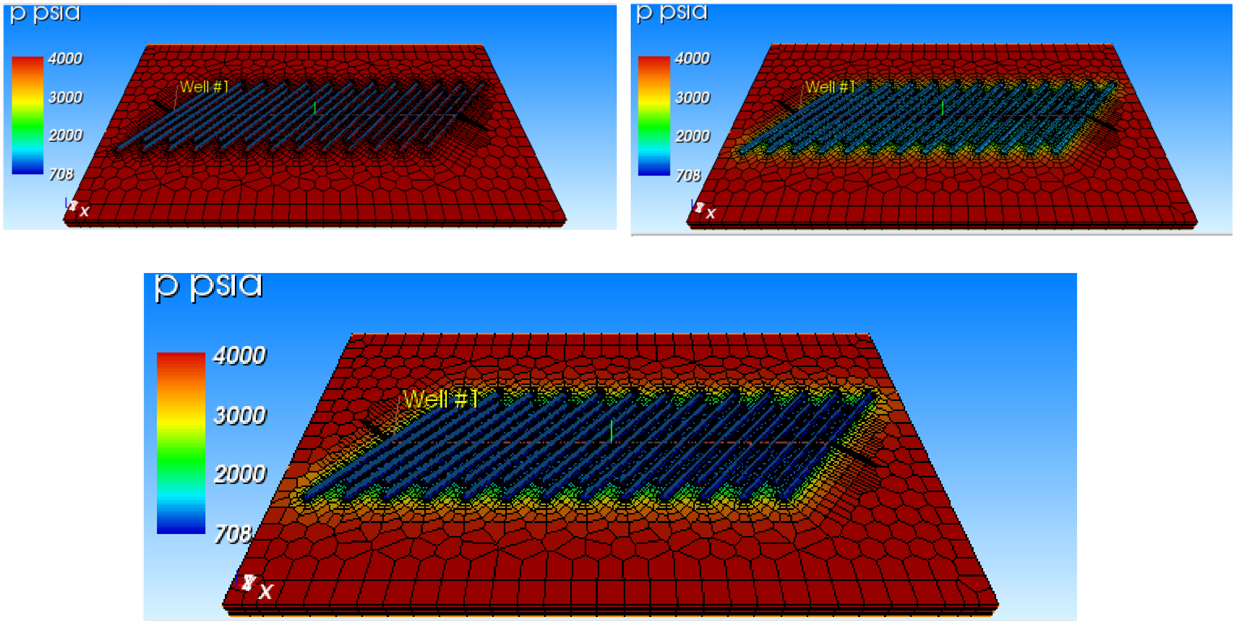

Figure 64: 3D pressure distribution maps before production, at time 6 years and at end of production (10 years) for case 7

Case 8

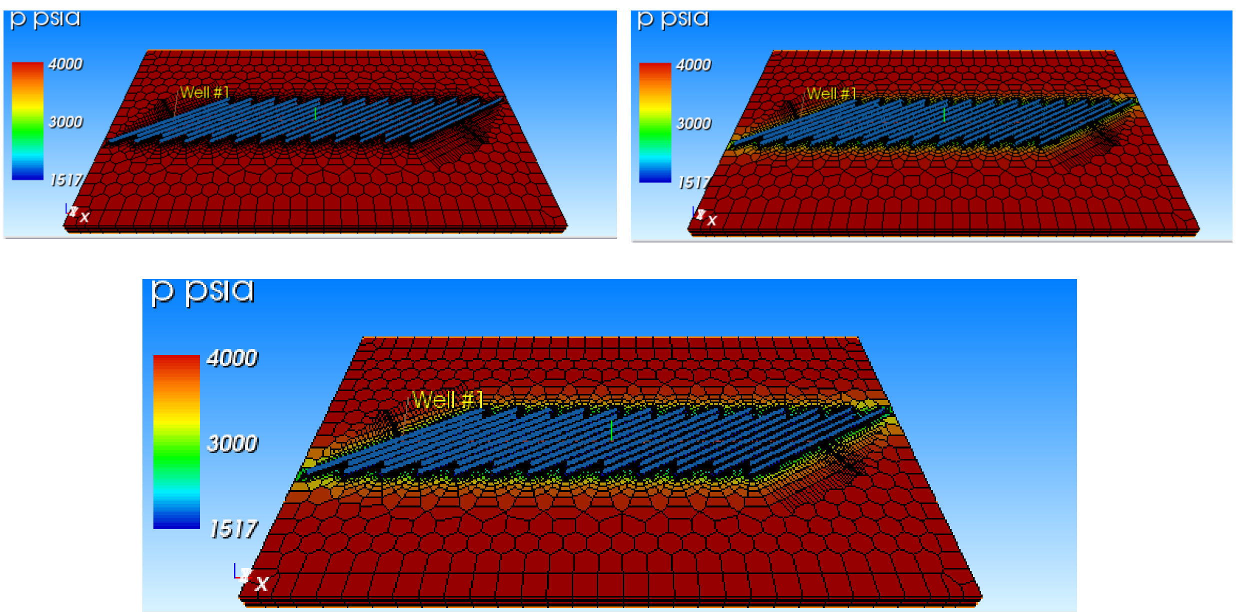

Figure 65:3D pressure distribution maps before production, at time 6 years and at end of production (10 years) for case 8

Case 9

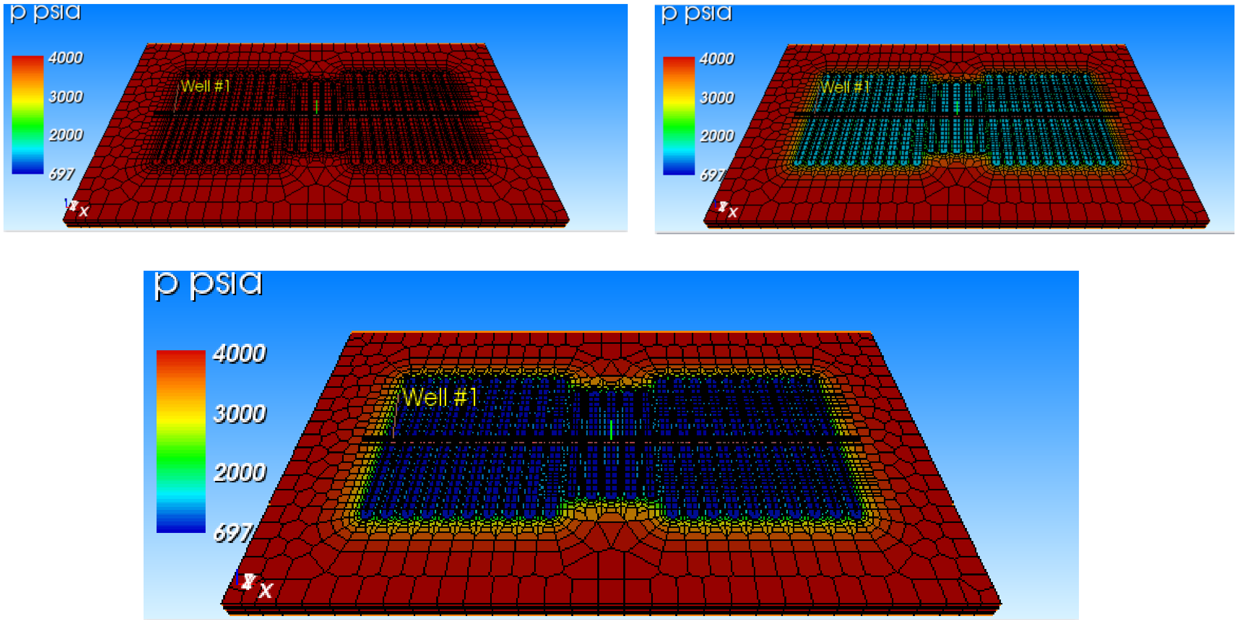

Figure 66:3D pressure distribution maps before production, at time 6 years and at end of production (10 years) for case 9

Case 10

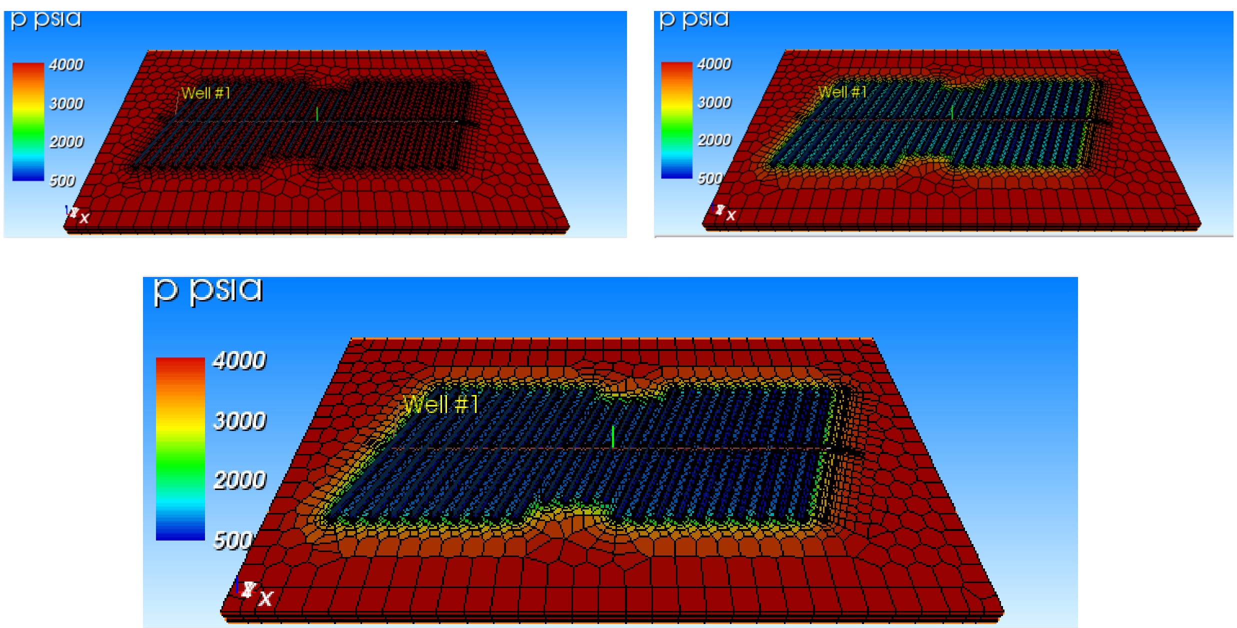

Figure 67:3D pressure distribution maps before production, at time 6 years and at end of production (10 years) for case 10

Case 11

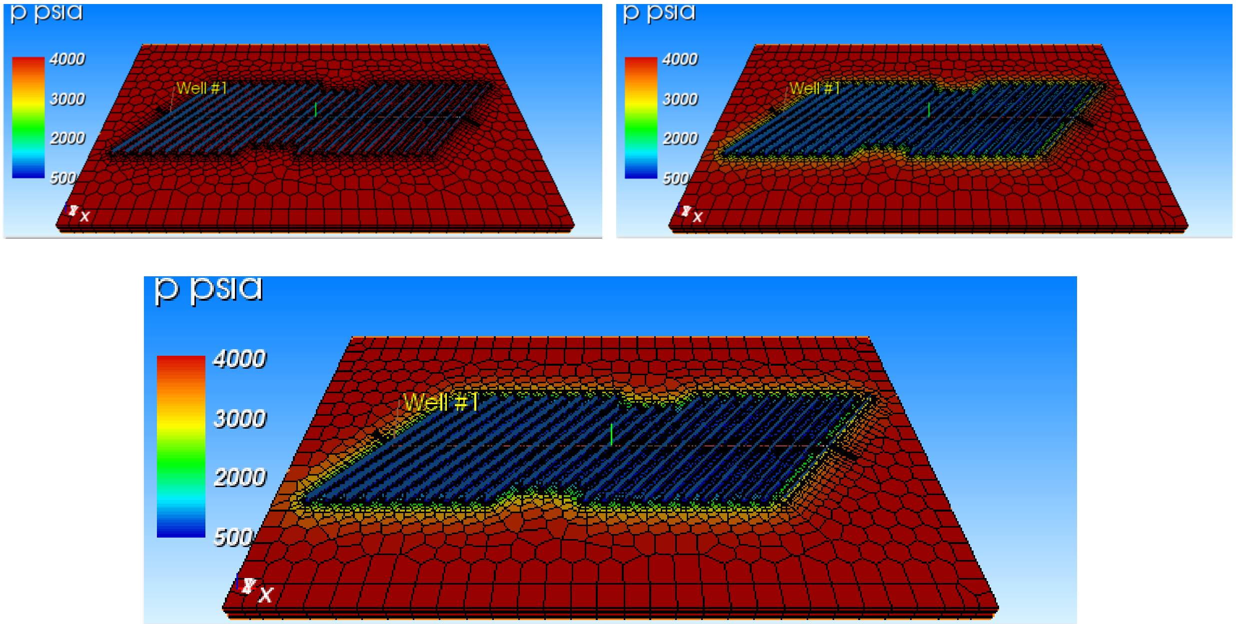

Figure 68: 3D pressure distribution maps before production, at time 6 years and at end of production (10 years) for case 11

Case 12

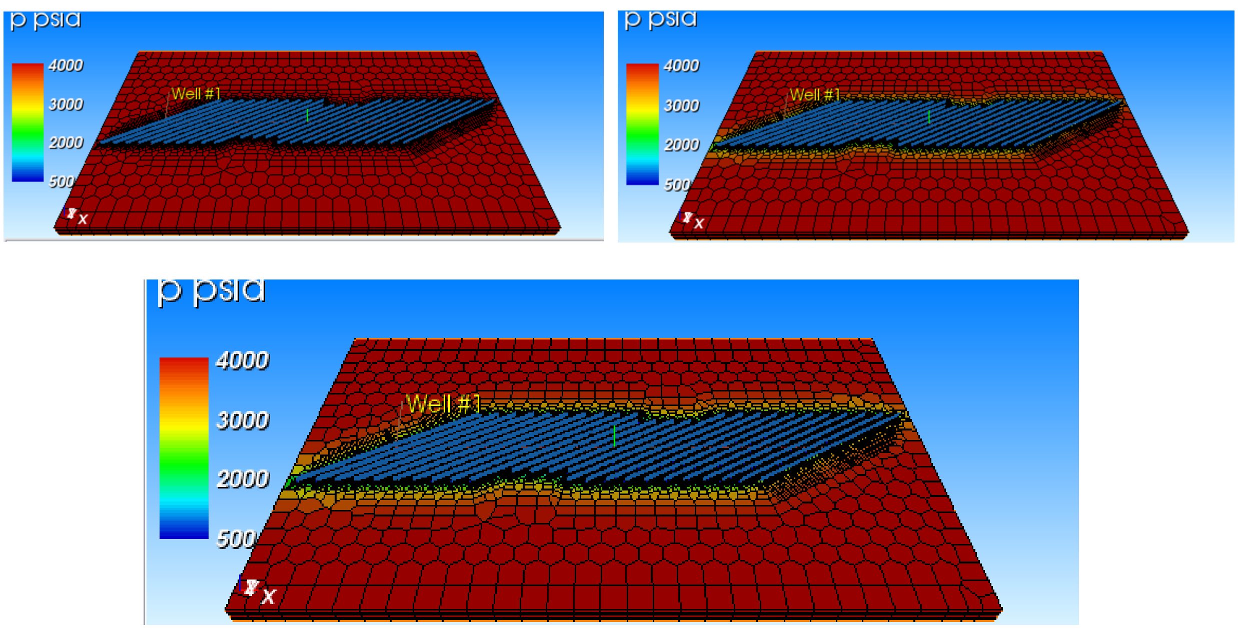

Figure 69:3D pressure distribution maps before production, at time 6 years and at end of production (10 years) for case 12

Case 13

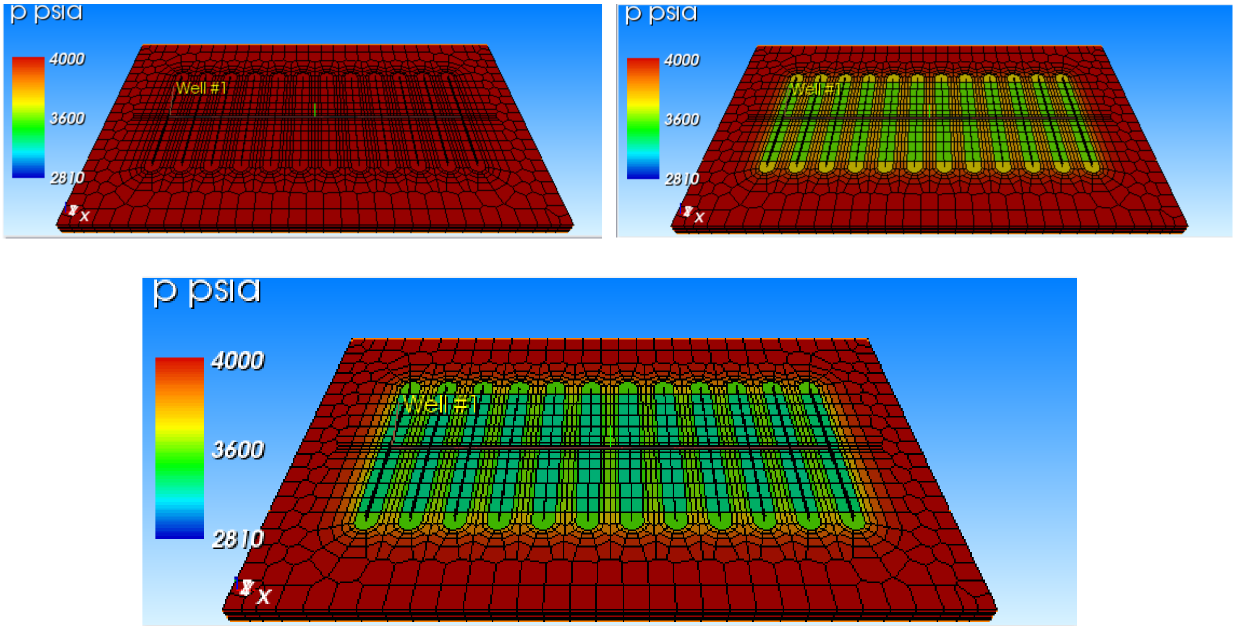

Figure 70:3D pressure distribution maps before production, at time 6 years and at end of production (10 years) for case 13

Case 14

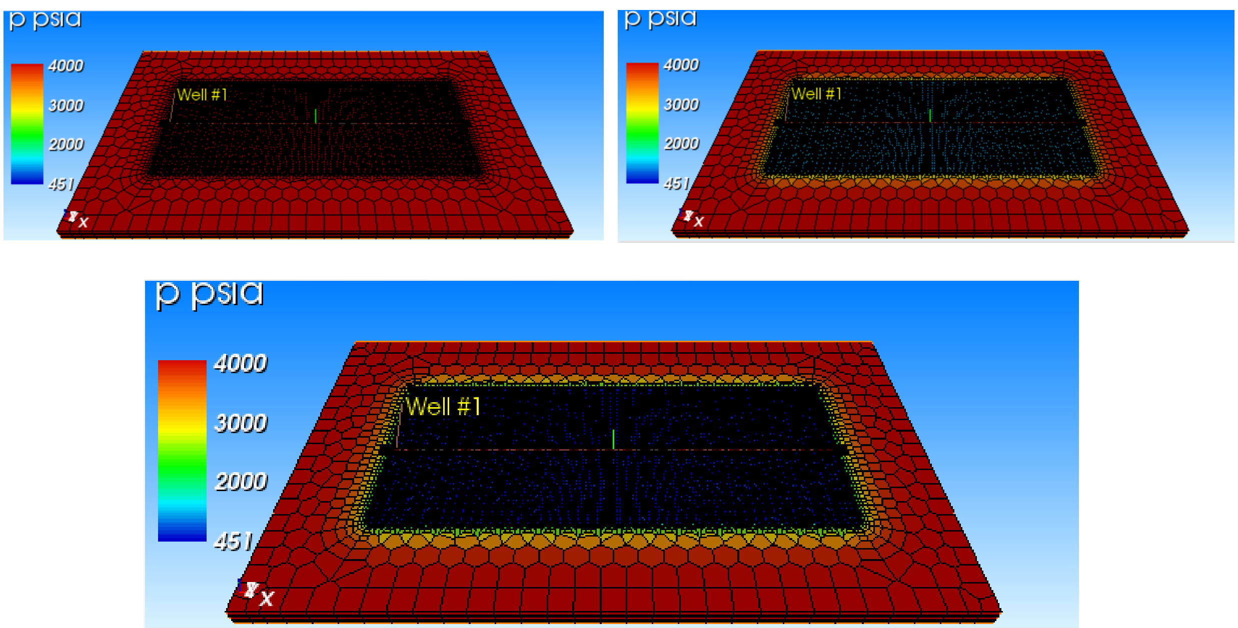

Figure 71: 3D pressure distribution maps before production, at time 6 years and at end of production (10 years) for case 14

Case 15

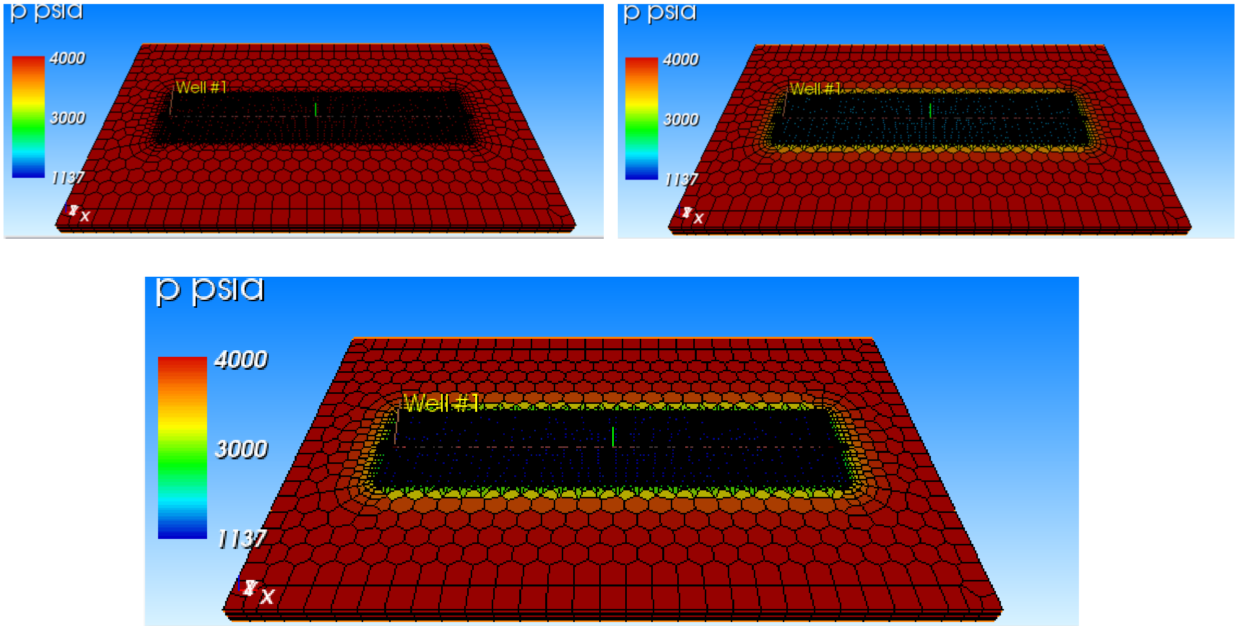

Figure 72:3D pressure distribution maps before production, at time 6 years and at end of production (10 years) for case 15

Case 16

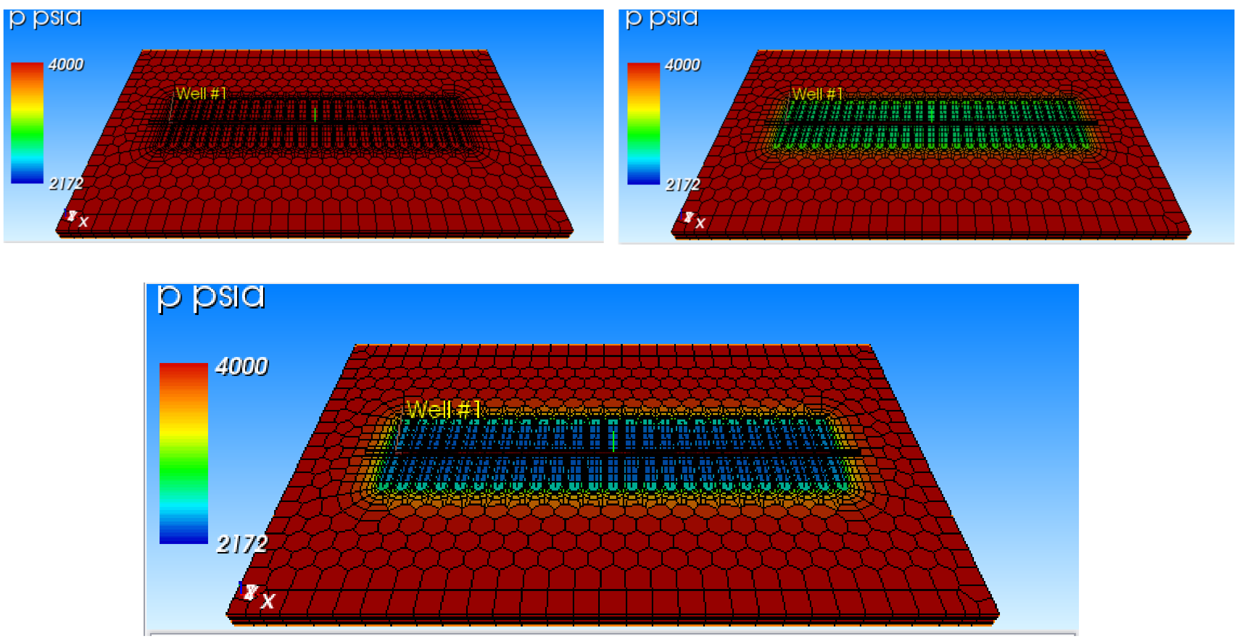

Figure 73:3D pressure distribution maps before production, at time 6 years and at end of production (10 years) for case 16

Case 17

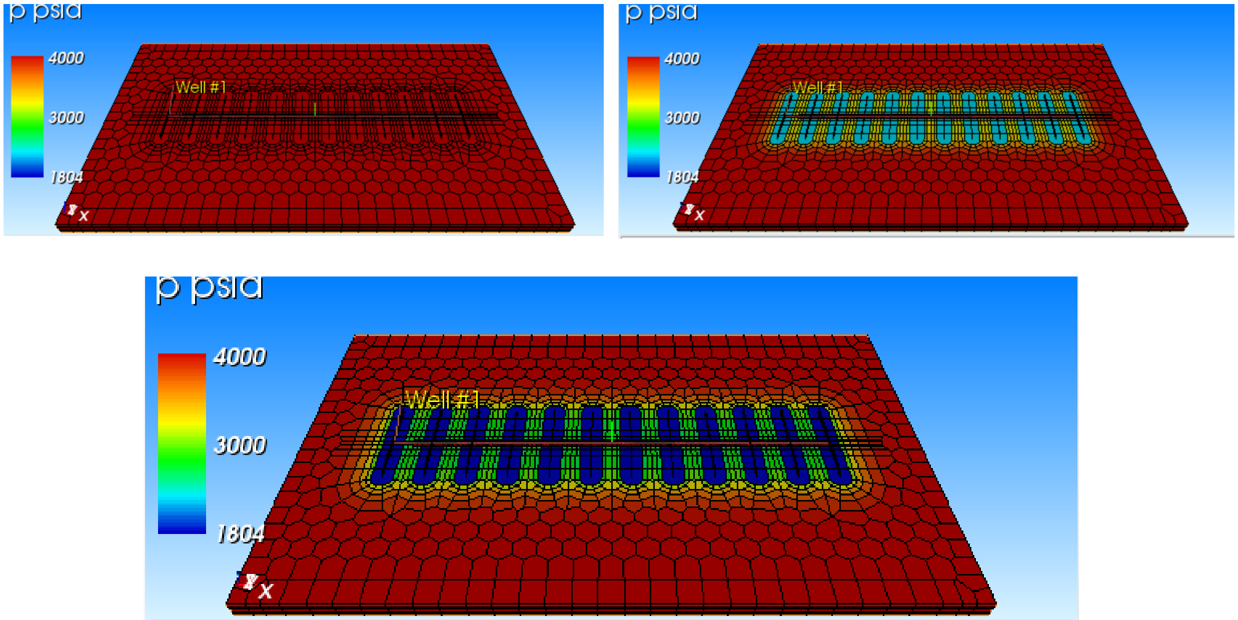

Figure 74:3D pressure distribution maps before production, at time 6 years and at end of production (10 years) for case 17

Case 18

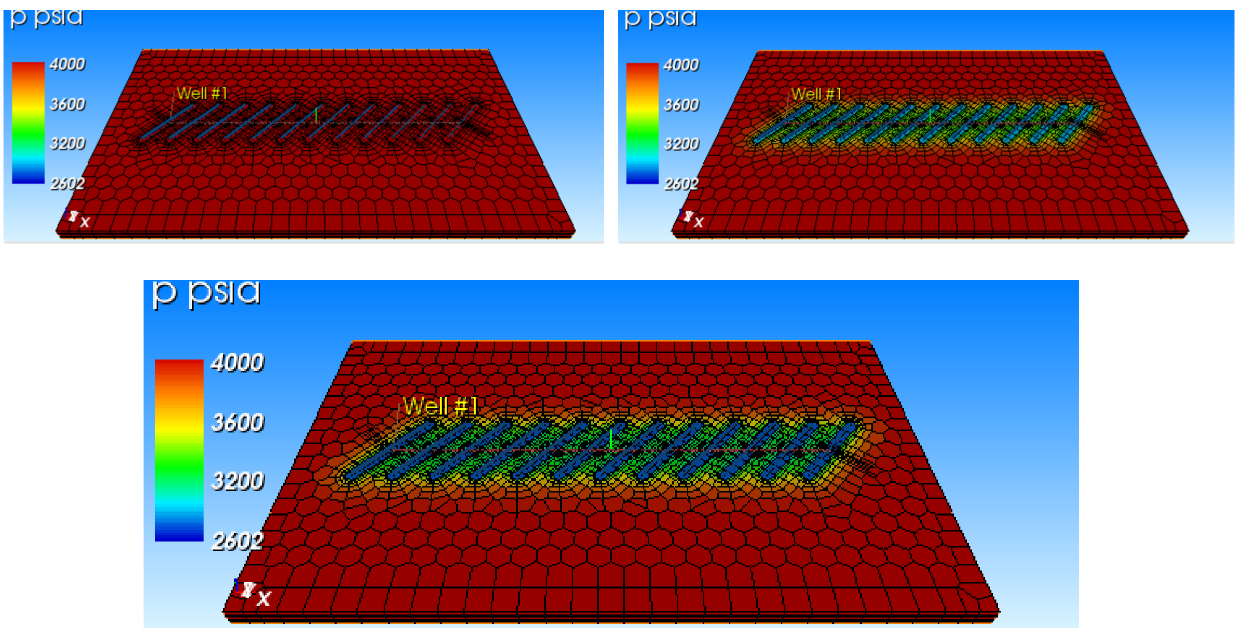

Figure 75:3D pressure distribution maps before production, at time 6 years and at end of production (10 years) for case 18

Case 19

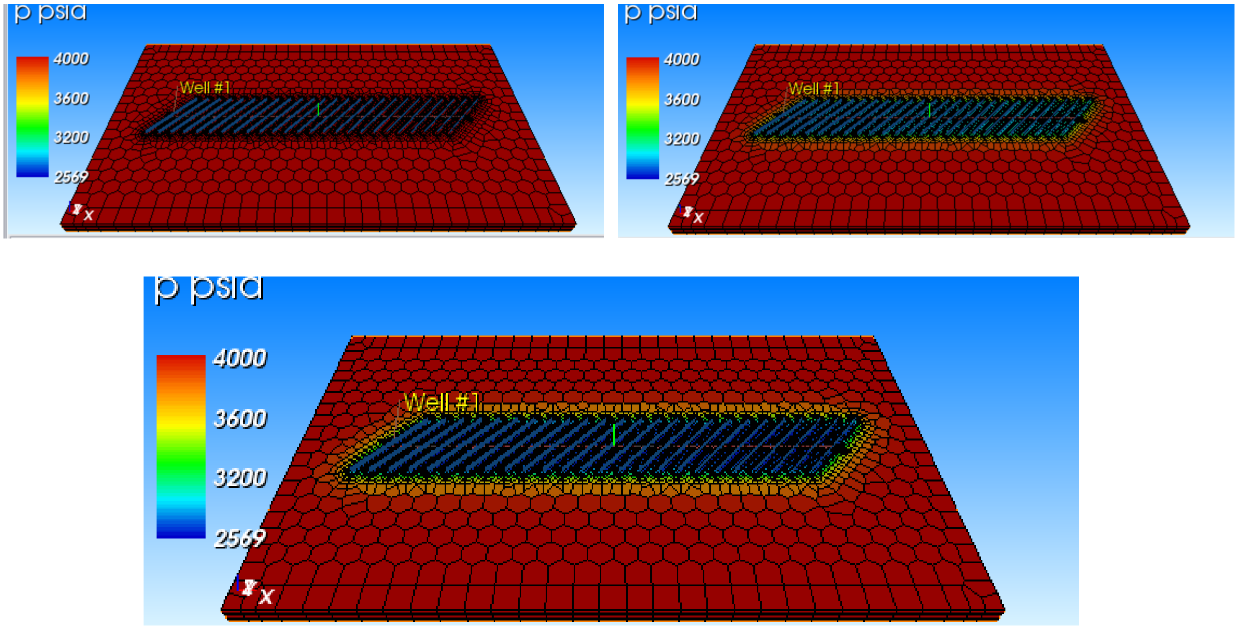

Figure 76:3D pressure distribution maps before production, at time 6 years and at end of production (10 years) for case 19

Case 20

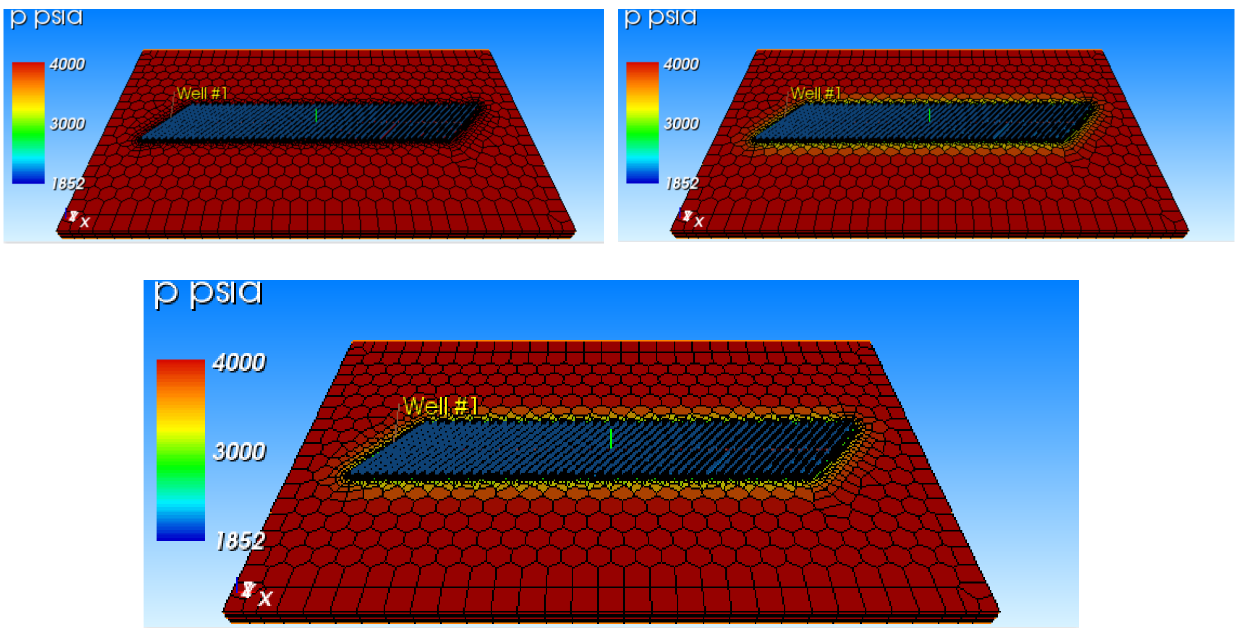

Figure 77:3D pressure distribution maps before production, at time 6 years and at end of production (10 years) for case 20

4.3 Dual-Phase Flow Cases

To further investigate the effect of a fracture's geometry on dual-phase flow, 3 more cases were obtained from a partner student (15). These cases simulated a reservoir with the same parameters as before, however using a more powerful simulator by Texas A&M University and the EDFM approach to reduce the computational power required. The reservoir had an initial water saturation Swi = 0.2 and the following relative permeability curves.

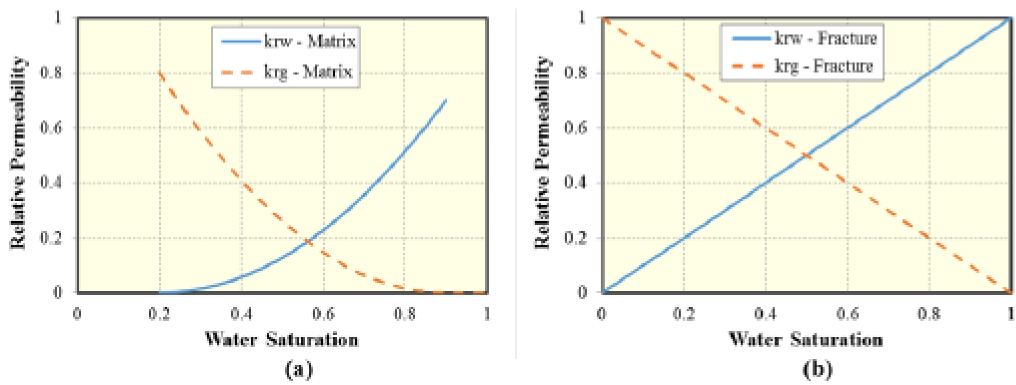

Figure 78: Relative Permeability Curves (15)

It should also be noted that the total length of the fractures for all the cases shown below as well as for a planar base/reference case was kept constant at 25,500ft. Moreover, the total amount of water injected was kept constant (SRV).

The three cases had the following geometries:

Irregular Case: Fractures follow a zigzag pattern with irregular lengths.

Fracture Network Case: A fracture network is created due to the fractures intersecting each other and adjacent fractures as well.

Random Case: Similar to the irregular case, however, differs in how far each fracture extends from the wellbore.

Irregular Case (15)

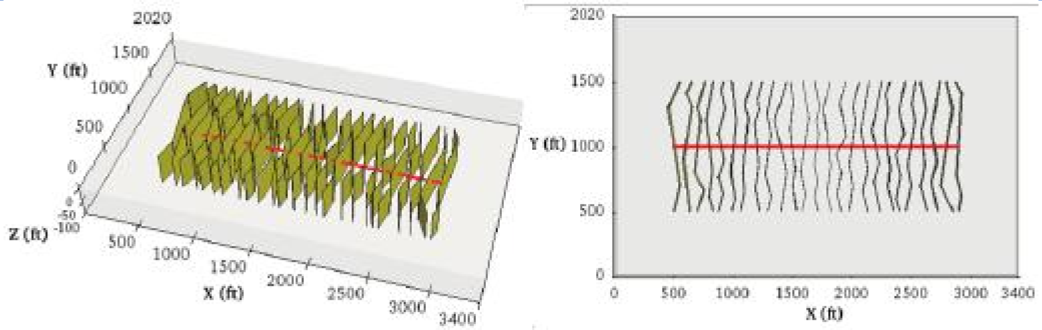

Fracture Network Case (15)

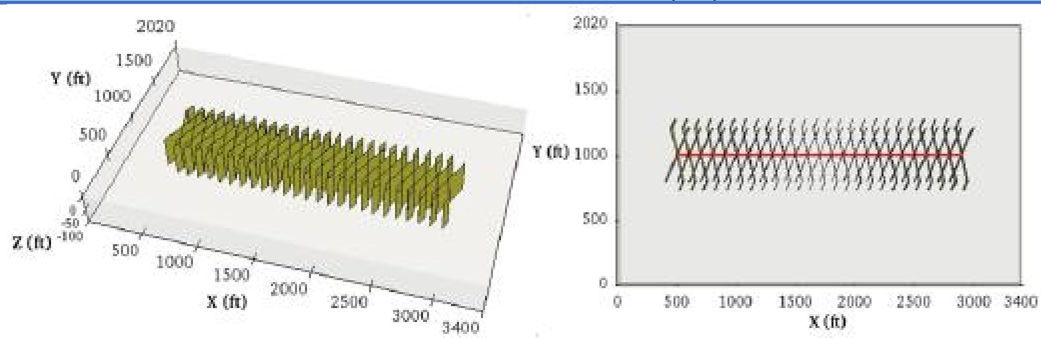

Random Case (15)

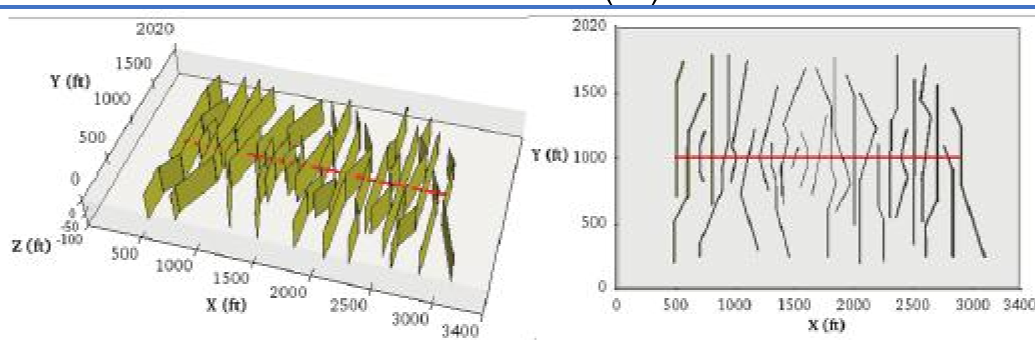

After running the simulation, both the cumulative gas production as well as cumulative water production were obtained. The following graphs display the results of the 3 cases as well as the reference case.

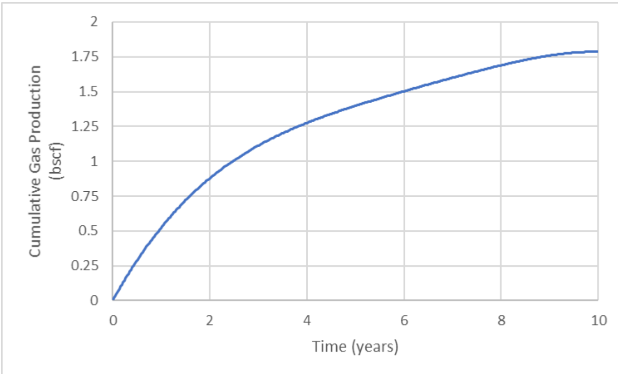

Figure 79: Cumulative Gas Production for Reference Case

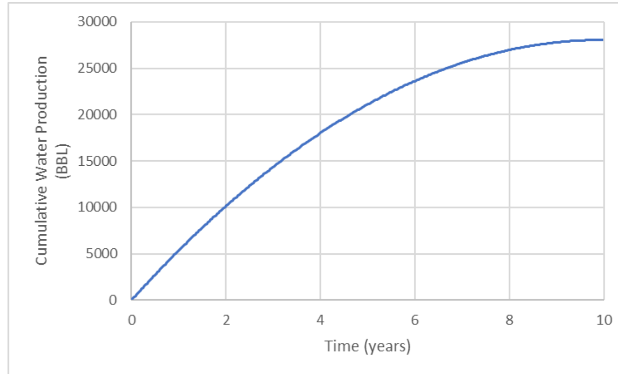

Figure 80: Cumulative Water Production for Reference Case

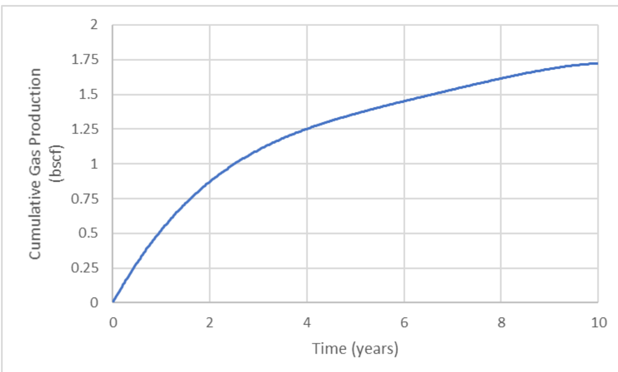

Figure 81: Cumulative Gas Production for Irregular Case

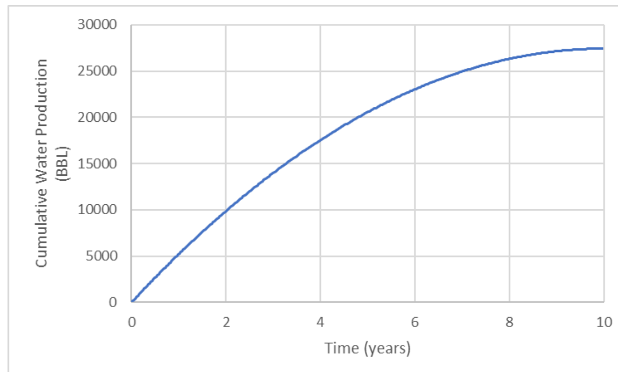

Figure 82: Cumulative Water Production for Irregular Case

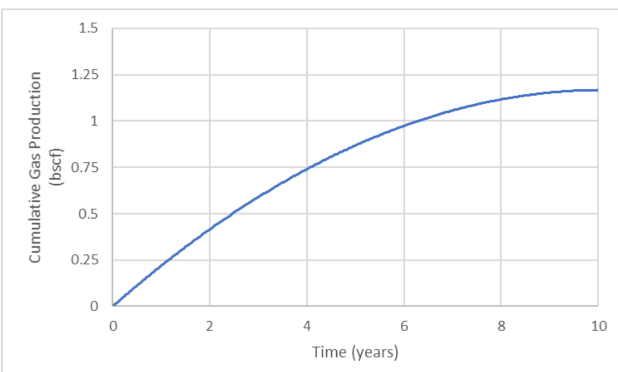

Figure 83:Cumulative Gas Production Fracture Network

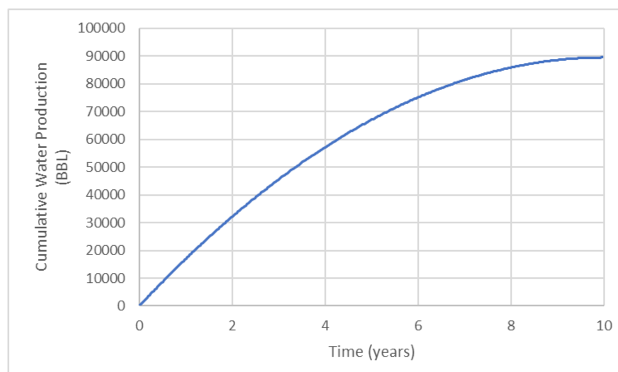

Figure 84:Cumulative Water Production Fracture Network

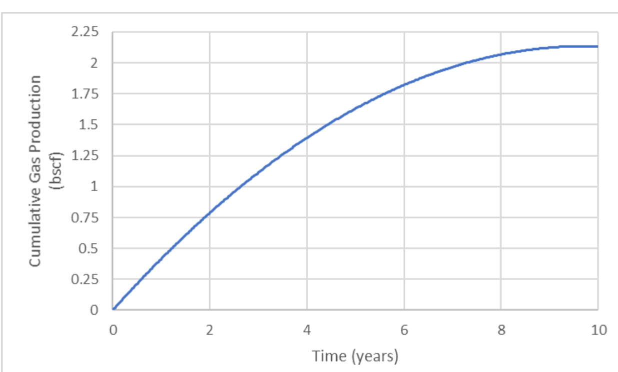

Figure 85: Cumulative Gas Production for Random Case

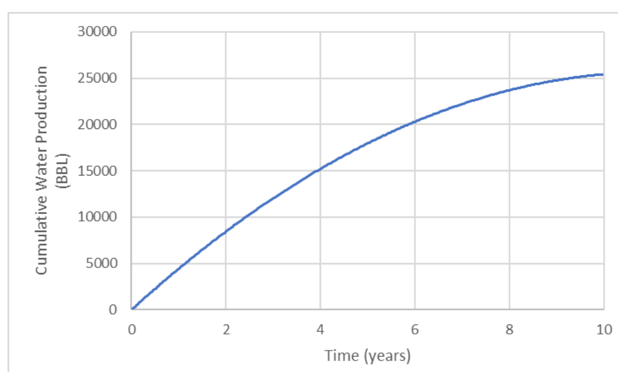

Figure 86:Cumulative Water Production for Random Case

	Reference	Irregular	Fracture Network	Random
Cumulative Gas Production at 10 Years (bscf)	1.8	1.74	1.15	2.1
% Change in Cumulative Gas Production at 10 years from the base case		-3%	-36%	17%

Table 7:Summary of Cumulative Gas Production (bscf) and the percentage change from the reference case at the end of the 10 years

Table 6 summarized the cumulative gas production at the end of the simulation period. It displays the amount at 10 years count for each case, then shows the percentage difference from the planar case.

As can be seen from the figures above, the cumulative gas production for the reference and irregular cases are somehow indifferent with only a 3% difference. Similarly, the cumulative water production is also indifferent with 7% only. This can be attributed to the fact that both cases create failry the same stimulated reservoir volume (SRV). In other words, even though each case had a different fracture geometry the rock volume stimulated by the fractures is somewhat similar. As a result, the two cases are exposed to the same drainage area and produce a very similar well performance.

The two other cases, however, produce a very different well performance. With the fracture network case producing 36% less gas in the 10 years simulation period. In fact, the fracture network produced the lowest amount of gas when compared to all the other cases. On the contrary, it had a water flowback of 92,000BBL at 10 years count; more than 220% more than the planar case making it the highest among all the other cases. The random case had the most promising results with a 17% increase in the amount of gas produced over the simulation period. When comparing the water production, it had the lowest among all other cases. The very huge difference in productivity of these two cases when compared to each other and to the planar case as well can be attributed to the difference in the stimulated reservoir volume (SRV). The random case having the largest SRV produced the highest amount of gas, while the fracture network case having the lowest SRV produced the least amount of gas.

Table 7 provides a summary of the cumulative water production over the 10-year simulation period, it also shows how much the difference is from the base case as a percentage. Finally, a RF is calculated assuming that only injected water flows back to the surface during the production cycle.

	Reference	Irregular	Fracture Network	Random
Cumulative Water Production at 10 Years (BBL)	28000	26000	92000	25000
% Change in Cumulative Water Production at 10 years from the base case		-7%	228%	-10%
% Recovery of Injected Water	2.8%	2.6%	9.2%	2.5%

Table 8: Summary of the Cumulative Water Production for each case, the percentage difference from the planar case and RF assuming only injected water flows back.

Three cases recovered almost the same amount of water, ranging from 2.5% till 2.8% for the planar, irregular and random case. The Fracture network case however, produced about 10% of the injected water as flow back. This can also be attributed to the SRV of each case. The fracture network case had the smallest stimulated reservoir volume size out of all cases. In other words, the injected water had a smaller volume of rock to imbibe and stimulate as compared to the other cases. So, when production in the well began, it is probable that a large amount of injected water was of proximity to the well and thus available flow-back. Another explanation to this can be due to the fractures' closer proximity, more due to interference caused by them intersecting one another. The fracture network resulted in a more pronounced interference between the fractures when compared to the other cases where the fractures' geometries were uniformly spaced, nonetheless never interested one another A high stimulated reservoir volume (SRV) on the other hand as can be seen for the random case resulted in much higher cumulative gas production. This can be due to the absence or minute presence of interference between the fractures for the random case.

4.3.1 Presence of Natural Fractures

To investigate the effect of the presence of natural fractures and their interaction with induced fractures, another level of complexity is added to the reservoir model. For this part of the study, only the random case, in terms of induced fractures, will be taken into consideration due to its extension from the horizontal wellbore and the higher probability of crossing the natural fractures with sets of 100 and 1000 natural fractures added to the reservoir alternating between either a 1-set orientation or a 2-set perpendicular orientation.

The table below summarizes the main properties of the natural fractures.

Parameter	Value	Unit
Natural fracture height	100	ft
Natural fracture length	100-300	ft
Natural fracture width	0.001	ft
Natural fracture conductivity	0.1	mD.ft
Natural fracture Dip angle	90	degrees
1-set orientation range	5-10	degrees
2-set orientation range	5-10 and 90-100	degrees

Table 9: Main parameters of the natural fractures (15)

The figures below display how each case of natural fractures is present in a 3D map of the reservoir.

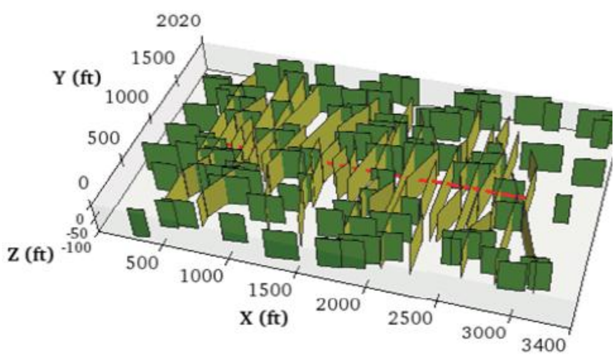

Figure 87: 1-set 100 natural fractures (15)

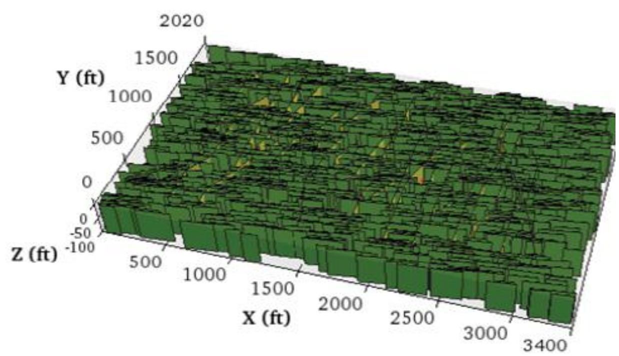

Figure 88: 1-set 1000 natural fractures (15)

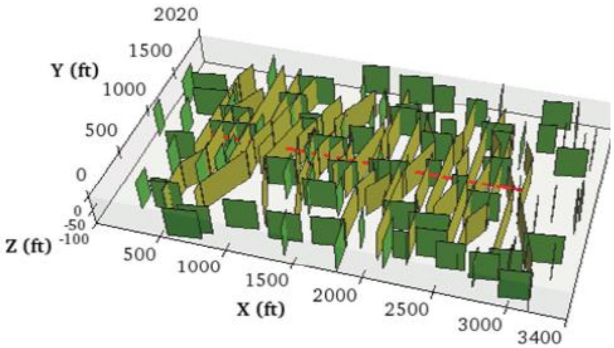

Figure 89: 2-set 100 natural fractures (15)

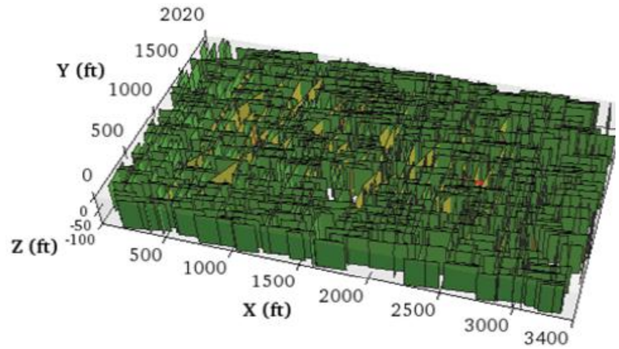

Figure 90: 2-set 1000 natural fractures (15)

After running the simulation for the 4 different cases of natural fractures considering a random induced fracture case, a graph comparing the cumulative gas production and the cumulative water production over the 10-year period was made. The natural fractures impacted the production considerably with very high percentages for some of the cases.

The two graphs below show the cumulative productions. It is noticeable that the more the natural fractures we have, the higher production for both gas and water is achieved.

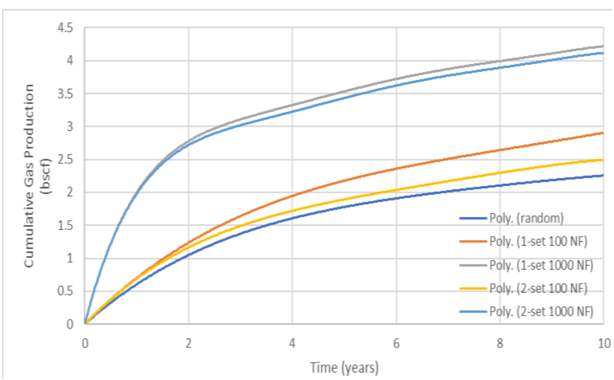

Figure 91: Comparison of the Cumulative Gas Production with Natural Fractures

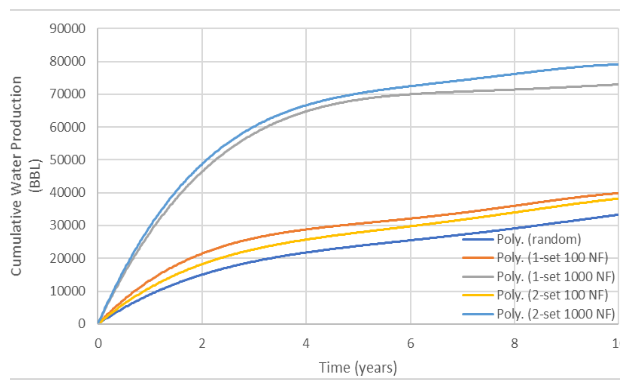

Figure 92: Comparison of Cumulative Water Production with Natural Fractures

	No natural fractures	1-set 100 NF	1-set 1000 NF	2-set 100 NF	2-set 1000 NF
Cumulative Gas Production (bscf) at 10 years	2.25	2.9	4.22	2.5	4.12
% Change from No NF		28%	87%	11%	83%

Table 10: Summary of the Cumulative gas production of the different cases of natural fractures with a percentage difference from no NF case

	No natural fractures	1-set 100 NF	1-set 1000 NF	2-set 100 NF	2-set 1000 NF
Cumulative Water Production (BBL) at 10 years	34000	41000	73000	39000	79000
% Change from No NF		20%	114%	14%	132%

Table 11: Summary of the Cumulative Water production of the different cases of natural fractures with a percentage difference from no NF case

The tables above display the enhancement in recovery of both gas and water in the presence of natural fractures. As a matter of fact, this enhancement was expected as the presence of natural fractures meant more exposure to the rock by the hydraulic fractures and thus a higher drainage area for the well. In short, presence of the natural fractures shows an opportunity for an enhanced recovery with more natural fractures resulting in a higher well productivity as well. It should be noted that the natural fractures for this model were assumed open and not sealed. Another factor that plays a role in the final recovery is the orientation of the natural fractures. A more favorable orientation is one that provides better intersection with the hydraulic fractures and since the orientation is governed by the state of stress in the shale rocks; a correct well placement is critical to take advantage of the largest drainage area possible.

As the results of both the graphs and tables show, a minor change in cumulative production was noticed for the 1-set and 2-set natural fractures with the highest change being 28% for 1-set 100 NF for cumulative gas production. However, when it came to the

1000 NF a considerable change in the cumulative production was noticed reaching a high percentage of 132 for 2-set 1000 NF for cumulative water production.

4.3.2 Effect of Varying Swi and Conductivity

A sensitivity analysis was conducted on the reservoir to study the effect of modifying the initial water saturation first in the fractures and the fractures' conductivity second. It should be noted that the sensitivity analysis was conducted for the planar base case only. The first analysis made tested 4 different Swi values which were 0.15, 0.25, 0.5 (the reference case) and finally 0.75. The Swi represent the initial water saturation in the fractures only whereas the matrix had a constant value of 0.2. The second analysis made was on the fractures' properties, specifically the fracture conductivity by varying it by factors of 10 from 0.1, 1, 10 and 100mD.ft (the reference case).

The table below summarizes the cumulative gas and water production at the end of the 10-year simulation period for the first sensitivity analysis of Swi providing the percentage difference from the original base case taken during the initial study.

Swi	**0.15**	**0.25**	**0.5***	**0.75**
Cumulative Gas Production at 10 Years (bscf)	3.4	3	1.8	0.7
% Change in Cumulative Gas Production from base case	83%	62%		-62%
Cumulative Water Production at 10 Years (BBL)	6000	8000	28000	112000
% Change in Cumulative Water Production from base case	-78%	-71%		300%

Table 12: Summary of the Cumulative gas and water production along with percentage difference at the end of the simulation period for different cases of initial water saturations

As can be seen from the results of the Swi sensitivity analysis, the cumulative gas production was affected the same for both cases of increasing Swi by half and decreasing by half with a 62% increase and decrease respectively. For the case of further reduction of Swi to 0.15 there wasn't a considerable change from the 0.25 case. When comparing the water flowback an Swi of 0.75 had about 300% increase in water flowback as compared to the reference case. While for the case of reducing Swi by half only 70% decrease in water production was detected, much like the 0.15 case with 78% decrease as well.

Fc (mD.ft)	0.1	1	10	100*
Cumulative Gas Production at 10 Years (bscf)	0.7	1.55	1.75	1.8
% Change in Cumulative Gas Production from base case	-61%	-14%	-3%	
Cumulative Water Production at 10 Years (BBL)	6800	16800	22600	28000
% Change in Cumulative Water Production from base case	-75%	-40%	-19%	

Table 13: Summary of the Cumulative gas and water production along with percentage difference at the end of the simulation period for different cases of fracture conductivities

The other sensitivity analysis made was to examine the effect of the fractures' conductivity on the overall well performance and the reservoir. As expected, the higher the conductivity in the fractures the higher both cumulative gas and water production was. Moreover, not much difference was detected for the high conductivities with only 3% and 19% difference from the base case for cumulative gas production and water flowback respectively. However, for the much smaller conductivities a huge difference was detected. With each decrease as a factor of 10 causing a significant change in the cumulative production. In other words, a major decline in the cumulative gas production was sought when the fracture conductivity went below 1mD.ft. on the other hand, in terms of water production, the decline in production was somehow consistent for each case.

Chapter 5: Conclusions and Recommendations

5.1 Conclusions

This research examines how a 3D shale gas reservoir model performs to different cases of hydraulic and natural fractures.

The first 20 cases examined the effect of fractures' angle from the horizontal wellbore (ranging from 90° to 30°), length and numbers on the well performance of single-phase gas flow. After running all the simulations, the following observations were made:

- ❖ The angle significantly affected how much gas was recovered. With each decrease in the angle resulting in a less cumulative gas production.
- ❖ In cases where the total fracture length was constant, it was observed that the angles of 70° and 50° produced similar results. This might be due to both cases having a similar stimulated reservoir volume . The 30° produced much smaller amounts of gas; this can be due to the outer fractures being of proximity to the reservoir's boundaries in the present case studies.
- ❖ As expected, decreasing the total fracture length had a negative effect on production; moreover, the fractures' angles had a higher effect for smaller half-lengths which can be due to heightened interference between the fractures.
- ❖ For the cases where the first few fractures had a smaller half-length the rest, a higher depletion was noticed in terms of pressure which produced higher amounts of gas during the initial year of production. However, as the pressure constraint of 500 psia was reached; the final cumulative production was like the base case.
- ❖ The last 8 single phase cases showed that doubling the number of fractures had a smaller effect than halving the number of fractures as the stimulated reservoir volume SRV changes drastically.
- ❖ The decrease in the fractures' half-length to half its initial value also caused the cumulative gas production to decrease more than 50% for the different number of fracture cases.

  In conclusion, the single phase flow cases proved that, for a constant total fracture length, not only the angle of a fracture has an effect on final recovery, but also how the fractures are distributed and spaced which shows to what extent interference between the fractures in a low permeability reservoir can influence recovery.

After that, a more complex study was conducted on dual-phase (gas and water) flow involving a simple planar reference case to more complex fracture geometries. These cases involved water injection before beginning the production in the well.

- ❖ The random case had the maximum cumulative gas production out of all other cases. However, its water production was similar to the other cases studies in comparison. This can be due to the fact that in the random case a non-uniform drainage area (non-uniform stimulated reservoir volume) was created by the hydraulic fractures. This, along with minimal interference between the fractures resulted in the high gas recovery.
- ❖ The planar and irregular cases had somewhat similar well performance in both gas and water recoveries. An explanation for this is that since both cases had a somewhat similar stimulated reservoir volume (drainage area) regardless of how complex or irregular the fracture geometries were, and the fracture's irregularity being on individual fractures at a time thus stimulating a similar reservoir volume; recoveries didn't differ by much.
- ❖ The fracture network case had the least gas recovery but the highest water recovery out of all cases. In the fracture network case, the fractures weren't uniformly spaced and intersected at multiple segments of the grid which resulted in a higher interference between the fractures. This coupled with a reduced SRV meant that more of the injected water was still in proximity of the production well resulting in a decrease in gas flow velocity and thus more water flowing back to the surface.

Another level of complexity was added to the reservoir model. This time by incorporating open natural fractures into the reservoir for the random case. These fractures were of different quantities and orientations. The following observations were made:

- ❖ The higher the number of natural fractures present, the higher the probability of interference/intersections between the hydraulic and natural fractures resulting in a larger stimulated reservoir volume. Thus, a much better recovery. In fact, when the number of natural fractures was multiplied by 10 (100NF vs 1000NF), recovery increased by 46% for 1-set natural fractures and by 65% for 2-set natural fractures.

- ❖ Another parameter taken into consideration was the orientation of the natural fractures. In fact, it was observed that the orientation that resulted in a higher amount of intersections between the hydraulic and natural fractures increased the overall recovery of the reservoir. As in real life these natural fractures depend on different factors, such as rock heterogeneity as well as in situ stress state, it is crucial to know how to place the well for utmost recovery.

Two further sensitivity analysis were made modifying the initial water saturation inside the fractures (SRV) initially then the fracture conductivity. The conclusion made is as follows:

- ❖ For the Swi, a higher Swi meant more cumulative water production as opposed to a lower gas recovery. So was the case for lower initial water saturations. However, it should be noted that after a specific increase or decrease in Swi the change doesn't hugely affect performance. This can be used as a chance to properly determine how much water should be injected into the reservoir for ultimate recovery.
- ❖ In the case of fracture conductivity, as expected the more we lower the conductivity the less recovery we obtain for both gas and water. However, for gas recovery a fracture conductivity less than 1 mD.ft resulted in a more pronounce decrease.

In summary, the results presented in this thesis have shown how important proper modeling of the induced hydraulic as well as natural fractures is in order to get a clearer view of the overall performance of the well. The heterogeneity of the induced fractures each result in a different stimulated reservoir volume depending on spacing, intersection and distribution which also affects the interference between individual fractures. The initial water saturation has also been shown to have an optimal value for an increased gas production while also having less water flow-back.

5.2 Recommendations

Reservoir modeling for 3D shale gas reservoirs and unconventional resources is constantly developing. This research paper shows a glimpse of how important it is to properly model fracture geometries and features for a better understanding of the overall well performance and recovery. However, more studies and more parameters should be incorporated for an even more accurate reservoir simulation. These recommendations are many and not only limited to the ones suggested below:

- Rock geomechanics can be integrated into the model as it can critically affect reservoir parameters such as permeability mainly due to the in-situ stresses (pressure) altering important shale rock parameters.
- An even more extensive modeling of the reservoir should be made. More seismic data should be collected after the stimulation of the reservoir to properly pay all micro-seismic events that happened in the reservoir. Thus, providing a much more accurate 3D map of the hydraulic fractures and their intersection with other natural fractures in the reservoir.
- More sensitivity analysis can be made for even more cases of hydraulic fracture complexities. Both reservoir and fracture parameters can be further modified to study the effect on the ultimate recovery of the reservoir.

Bibliography

1. **World Shale Resource Assessments. [Online] https://www.eia.gov/analysis/studies/worldshalegas/.**

2. EIA Proven Gas Reserves. [Online] https://www.eia.gov/beta/international/data/browser/#/?pa=000000000000000000004&c=ruvvvvvfvtvnvv1urvvvvfvvvvvvfvvvou20evvvvvvvvvnvvuvo&ct=0&tl_id=3002-A&vs=INTL.3-6-AFG-TCF.A&cy=2014&vo=0&pin=a&v=H.

3. Shale gas production drives world natural gas production growth. [Online] https://www.eia.gov/todayinenergy/detail.php?id=27512.

4. Energy Essentails . *Energy Institute .* [Online] [Cited: 8 June 2018.] https://knowledge.energyinst.org/__data/assets/pdf_file/0020/124544/Energy-Essentials-Shale-Gas-Guide.pdf.

5. Jordan Hanania, Kailyn Stenhouse, Jason Donev. Unconventional resource. *Unconventional resource.* [Online] http://energyeducation.ca/encyclopedia/Unconventional_resource.

6. Schlumberger. OilField Glossary. [Online] Schlumberger. [Cited: 16 November 2018.] www.glossary.oilfield.slb.com/en/terms/u/unconventional_resource.aspx.

7. Euzen, Tristan. *Shale Gas: An Overview.* s.l. : IFP Technologies (Canada) Inc, 2011. 10.13140/RG.2.1.2236.6242.

8. S, Drake. *Unconventional Gas Plays .* s.l. : American Association of Professional Landmen, 2007.

9. Energy Minerals Division. *Gas Shales.* s.l. : American Association of Petroleum Geologists, 2010.

10. *About technical terms of oil shale and shale oil.* Reinsalu, Enno and Aarna, Indrek. 4, s.l. : Estonian Academy Publishers, 2015, Vol. 32. ISSN 0208-189X.

11. Y, Cheng. Impact of Water Dynamics in Fractures on the Performance of Hydraulically Fractured Wells in Gas-Shale Reservoirs. [Online] 2012. [Cited: 18 November 2018.] http://dx.doi.org/10.2118/127682-PA. SPE-127863-PA.

12. C, Cipolla. Modelling Well Performance in Shale-Gas Reservoirs. [Online] 2009. [Cited: 18 November 2018.] http://dx.doi.org/10.2118/125532-MS. SPE-125532-MS.

13. L, Weijers. *The newar-wellbore geometry of hydraulic fracture initiated from horizontal and deviated wells .* s.l. : Delft Univerty of Technology, 1995.

14. *Impact of Shale gas production apparent permeability on production: combined effects of non-darcy flow/gas-slippage, desorption and geomechanics.* H, Wang and Marongui-Porcu. 04, s.l. : Society of Petroleum Engineers, 2015, Vol. 18. SPE-173196-PA.

15. AlTawaijri, Mohammad Hamad. *A Comprehensive Numerical Model for Simulating Two-Phase Flow in Shale Gas Reservoirs with Complex Hydraulic and Natural Fractures.* 2017.

16. Schlumberger. OilField Glossary. [Online] Schlumberger. [Cited: 16 November 2018.] www.glossary.oilfield.slb.com/en/terms/t/thermal_maturity.aspx.